UNIVERSIDAD DE BARCELONA

Facultad de Farmacia

Departamento de Bioquímica y Biología Molecular

# REDESIGN OF CARNITINE ACETYLTRANSFERASE SPECIFICITY BY PROTEIN ENGINEERING

**ANTONIO FELIPE GARCIA CORDENTE**

**2006**

# PUBLICATIONS

THE JOURNAL OF BIOLOGICAL CHEMISTRY

Vol. 279, No. 32, Issue of August 6, pp. 33899–33908, 2004
*Printed in U.S.A.*

# Redesign of Carnitine Acetyltransferase Specificity by Protein Engineering*

Received for publication, March 9, 2004, and in revised form, May 18, 2004
Published, JBC Papers in Press, May 21, 2004, DOI 10.1074/jbc.M402685200

**Antonio G. Cordente‡§, Eduardo López-Viñas¶‖, María Irene Vázquez‡**, Jan H. Swiegers‡‡, Isak S. Pretorius‡‡, Paulino Gómez-Puertas¶, Fausto G. Hegardt‡§§, Guillermina Asins‡, and Dolors Serra‡**

*From the ‡Department of Biochemistry and Molecular Biology, School of Pharmacy, University of Barcelona, Diagonal 643, E-08028 Barcelona, Spain, ¶Bioinformatics Laboratory (Centro de Astrobiologia/Consejo Superior de Investigaciones Cientificas), Torrejón de Ardoz, E-28850 Madrid, Spain, and ‡‡The Australian Wine Research Institute, P. O. Box 197, Glen Osmond, Adelaide SA-5064, Australia*

**In eukaryotes, L-carnitine is involved in energy metabolism by facilitating β-oxidation of fatty acids. Carnitine acetyltransferases (CrAT) catalyze the reversible conversion of acetyl-CoA and carnitine to acetylcarnitine and free CoA. To redesign the specificity of rat CrAT toward its substrates, we mutated $Met^{564}$. The M564G mutated CrAT showed higher activity toward longer chain acyl-CoAs: activity toward myristoyl-CoA was 1250-fold higher than that of the wild-type CrAT, and lower activity toward its natural substrate, acetyl-CoA. Kinetic constants of the mutant CrAT showed modification in favor of longer acyl-CoAs as substrates. In the reverse case, mutation of the orthologous glycine ($Gly^{553}$) to methionine in carnitine octanoyltransferase (COT) decreased activity toward its natural substrates, medium- and long-chain acyl-CoAs, and increased activity toward short-chain acyl-CoAs. Another CrAT mutant, M564A, was prepared and tested in the same way, with similar results. We conclude that $Met^{564}$ blocks the entry of medium- and long-chain acyl-CoAs to the catalytic site of CrAT. Three-dimensional models of wild-type and mutated CrAT and COT support this hypothesis. We show for the first time that a single amino acid is able to determine the substrate specificity of CrAT and COT.**

Carnitine acyltransferases are essential for the β-oxidation of fatty acids and thus play an important role in energy metabolism in eukaryotes. There are three carnitine acyltransferase families: the carnitine palmitoyltransferases (CPTs),[1] CPT I and CPT II, are essential for mitochondrial β-oxidation and are located in the outer and inner mitochondrial membrane, respectively. CPT I facilitates the transfer of long-chain fatty acids from the cytoplasm to the mitochondrial matrix, which is the rate-limiting step in β-oxidation (1). Mammalian tissues express three isoforms of CPT I (each encoded by a different gene), in liver (L-CPT I), muscle (M-CPT I) and brain (CPTI-c) (2–4). Carnitine octanoyltransferase (COT) facilitates the transport of medium-chain fatty acids from peroxisomes to mitochondria through the conversion of acyl-CoAs, shortened by peroxisomal β-oxidation, into acylcarnitine (5). Carnitine acetyltransferase (CrAT) catalyzes the reversible conversion of acetyl-CoA and carnitine to acetylcarnitine and free CoA.

Due to the impermeability of organelle membranes to CoA, CrATs function in a compartmental buffering system by maintaining the appropriate levels of acetyl-CoA and CoA in cellular compartments. In peroxisomes they remove excess activated acetyl groups releasing free CoA, which can then accept more acetyl groups produced by β-oxidation, thereby allowing the oxidation to proceed. This indirectly facilitates the transport of acetyl moieties to the mitochondria for oxidation (6, 7). Mitochondrial CrAT plays a major role in modulating matrix acetyl-CoA concentration. The production and utilization of acetyl-CoA in the mitochondrial matrix lie at a major metabolic crossroads. Regulation of the fate of acetyl-CoA is mediated, to a large extent, by the effects of the molecule itself on pyruvate dehydrogenase kinase, which is inhibited by a high acetyl-CoA/CoA ratio. In the liver, mitochondrial acetyl-CoA also activates the key gluconeogenic enzyme pyruvate carboxylase. Therefore, high rates of β-oxidation of fatty acids result in the activation of gluconeogenesis from pyruvate and its precursors. In mammalian tissues, CrATs can also contribute to the excretion of excess or harmful acyl molecules, such as acylcarnitines. CrAT activity has also been implicated in the cell cycle from $G_1$ to S phase (8). CrATs also appear to play an important role in human health. For example, decreases in CrAT activity have been reported in patients with disorders of the nervous system, such as Alzheimer's disease (9, 10), ataxic encephalopathy (11), and several vascular diseases (12, 13).

The crystal structures of the mouse and human CrAT have recently been reported, alone and complexed with their substrates carnitine or CoA (14, 15). The data provide critical insights into the molecular basis for acyl-chain transfer and a

* This study was supported in part by Grants BMC2001-3048 from the Dirección General de Investigación Científica y Técnica, by Grant C3/08 from the Fondo de Investigación Sanitaria of the Instituto de Salud Carlos III, Red de Centros en Metabolismo y Nutrición from the Ministry of Health, Madrid, Spain, by the Ajut de Suport als Grups de Recerca de Catalunya (2001SGR-00129), Spain, and by a grant from the Fundación Ramón Areces. The costs of publication of this article were defrayed in part by the payment of page charges. This article must therefore be hereby marked "*advertisement*" in accordance with 18 U.S.C. Section 1734 solely to indicate this fact.

*The atomic coordinates and structure factors (codes 1NM8 and INDB) have been deposited in the Protein Data Bank, Research Collaboratory for Structural Bioinformatics, Rutgers University, New Brunswick, NJ (http://www.rcsb.org/).*

*The nucleotide sequence(s) reported in this paper has been submitted to the GenBank™/EBI Data Bank with accession number(s) AJ620886.*

§ Recipient of a fellowship from the Generalitat de Catalunya.

‖ Recipient of a fellowships from the Fundación Ramón Areces.

** Recipient of a fellowship from the Ministry of Science and Technology.

§§ To whom correspondence should be addressed. Tel.: 34-93-402-4523; Fax: 34-93-402-4520; E-mail: fgarciaheg@ub.edu.

[1] The abbreviations used are: CPT, carnitine palmitoyltransferase; COT, carnitine octanoyltransferase; CrAT, carnitine acetyltransferase; wt, wild-type; nt, nucleotide(s); GST, glutathione *S*-transferase.

possible common mechanism for all carnitine acyltransferases. A histidine residue interacts with an aspartic/glutamic acid at the catalytic site (16) and acts as a general base (1). The position of this histidine at the center of the catalytic tunnel allows access to both substrates carnitine and acetyl-CoA, which lie on opposite sides of the tunnel (15, 17). The catalytic His extracts the proton from the 3-hydroxyl group of carnitine or the thiol group of CoA, depending on the direction of the reaction. The activated hydroxyl or thiol group then has direct access to the carbonyl carbon in acyl-CoA or acylcarnitine, and the reaction proceeds without the formation of an acyl-enzyme intermediate (14). Previous site-directed mutagenesis experiments have demonstrated an essential catalytic role for the homologous histidines in CPT II, L-CPT I, and COT (16, 18, 19).

Substrate specificity of carnitine acyltransferases may be a function of structural features that govern the fit of the carbon chain. The acetyl group of acetylcarnitine points toward a hydrophobic pocket in the CrAT crystal, which is located at the intersection of the two beta sheets in the enzyme (14). In CrAT, this pocket is partly occupied by the side chain of $Met^{564}$. Because the equivalent residue in all other carnitine acyltransferases is a glycine, $Met^{564}$ could be the residue that blocks the access of medium- and long-chain fatty acids to the hydrophobic pocket.

Here we report site-directed mutagenesis that modified CrAT $Met^{564}$ to glycine, its counterpart in COT, CPT I and CPT II. We assessed the kinetic properties of the yeast-expressed mutant for acyl-CoA substrates other than acetyl-CoA. Catalytic efficiency and enzyme activity of the mutant favored longer acyl-CoAs. Moreover, we also mutated COT $Gly^{553}$ (orthologous to CrAT $Met^{564}$) to methionine. The activity of the COT mutant G553M toward several acyl-CoAs was practically identical to wt CrAT. Docking analyses on the three-dimensional models of wt and mutated CrAT and COT confirm that $Met^{564}$ blocks the entry of the hydrocarbon chain of acyl-CoAs to the CrAT molecule.

## EXPERIMENTAL PROCEDURES

*Cloning of Rat CrAT*—Rat CrAT cDNA was amplified by PCR, using the *Pfu*Turbo® DNA polymerase (Stratagene), from rat testis cDNAs using two primers: CrATATG.for (5′-ATGTTAGCTTTTGCTGCCAG-3′) and CrAT2100.rev (5′-CTTGTTCAGCCTCTGGGCTCAGC-3′). The former was taken from a rat CrAT DNA sequence (XM_242301) and contains the ATG start codon, and the latter was designed from a rat cDNA clone that corresponds to the 3′-untranslated region of rat CrAT (GenBank AA925306). A fragment of 2070 nucleotides was obtained, purified, and subcloned into the pGEM®-T vector (Promega), yielding the pGEM-T-$CrAT^{wt}$ construct. The rat CrAT cDNA fragment was sequenced (GenBank AJ620886) with an Applied Biosystems 373 automated DNA sequencer.

*Construction of the Rat CrAT and COT Models*—The structural models for wt CrAT and wt COT were constructed using homology modeling procedures based on the multiple, structure-based alignment of the rat CrAT and COT amino acid sequences with members of the carnitine acyltransferase family, including the three-dimensional structures of human CrAT (Protein Data Bank (PDB) entry 1NM8 (15)) and mouse CrAT (free enzyme structure: PDB accession number 1NDB; carnitine complex: 1NDF; CoA complex: 1NDI (14)). The three-dimensional models were built using the program Swiss-Pdb Viewer and the SWISS-MODEL server facilities (20–23) (available at www.expasy.ch/swissmod/SWISS-MODEL.html). The structural quality was checked using the WHAT-CHECK routines (24) from the WHAT IF program (25) and the PROCHECK validation program from the SWISS-MODEL server facilities (26); briefly, the quality values of both models are within the range expected for protein structural models. The three-dimensional models of CrAT mutants M564G and M564A and COT mutant G553M were built by the same procedures using the structures obtained for the respective wt enzymes as templates.

*Molecular Docking*—Docking calculations to obtain a molecular model of the interaction between the substrates acetyl-CoA, decanoyl-CoA, and myristoyl-CoA and the three-dimensional models of the putative receptor proteins wt CrAT, wt COT, CrAT M564G, M564A, and COT G553M were performed using the programs Autodock (27, 28) and Hex (29). Protein targets and ligands (acyl-CoAs and carnitine) were prepared using the algorithms Addsol and Autotors from the Autodock package. For each individual calculation, a global search (100 cycles) was performed using Autogrid and Autodock. Having discarded the non-realistic positions far from the substrate cavity described for acetyl-CoA in the PDB 1NDI crystal structure, the ligand positions of lowest energy were selected. The relative positions of the acyl extensions of the ligand molecules were refined using the rigid docking program Hex.

*Construction of Plasmids For Expression in Saccharomyces cerevisiae*—For expression experiments on CrAT, the 1925-nt fragment containing the rat CrAT coding region was subcloned into the *S. cerevisiae* expression plasmid pYES2 (Invitrogen). To enable cloning into the only HindIII site of the pYES2 plasmid, a HindIII site (underlined in the HindIII-CrAT.for primer) immediately 5′ of the ATG start codon was introduced by PCR, using pGEM-T-$CrAT^{wt}$ as template. A consensus sequence (in boldface type), optimized for efficient translation into yeast, was also introduced in the same PCR, using the forward primer HindIII-CrAT.for (5′-TCGAT<u>AAGCTT</u>**ATAAA**ATGTTAGCCTTTGCTGCCAGAAC-3′) and the reverse primer EcoRICrAT.rev (5′-CG<u>GAATTC</u>CGCCAAAGTGGGCTTGGCTGTG-3′), which introduces a HindIII and EcoRI sites (underlined). PCR products were digested with HindIII and EcoRI and ligated to the pYES2 plasmid, producing pYES$CrAT^{wt}$. For protein expression experiments on COT, plasmid pYES$COT^{wt}$ was prepared as described elsewhere (19).

*Construction of Plasmids for Expression in Escherichia coli*—To express the rat CrAT protein in *E. coli*, a cDNA fragment containing CrAT was obtained from plasmid pYES$CrAT^{wt}$, digested with HindIII, blunt-ended, and again digested with EcoRI. This fragment was then purified and subcloned into the expression vector pGEX-6P-1 previously digested with BamHI, blunt-ended, and again digested with EcoRI. The plasmid obtained was pGEX-$CrAT^{wt}$.

*Construction of Site-directed Mutants*—CrAT mutants M564G, M564A, H343A, and E347A were constructed using the QuikChange PCR-based mutagenesis procedure (Stratagene) with the pYES$CrAT^{wt}$ plasmid as template. COT mutant G553M was constructed using pYES$COT^{wt}$ as template. The following primers were used: primer CrATM564G.for (5′-CAAGACAGACTGTGTC<u>GG</u>GTCCTTCGGACCTGTG-3′), and primer CrATM564G.rev (5′-CACAGGTCCGAAGGAC<u>CC</u>GACACAGTCTGTCTTG-3′) were used to construct pYES$CrAT^{M564G}$; primer CrATM564A.for (5′-CAAGACAGACTGTGTC<u>GC</u>GTCCTTCGGACCTGTG-3′), and primer CrATM564A.rev (5′-CACAGGTCCGAAGGAC<u>GC</u>GACACAGTCTGTCTTG-3′) were used to construct pYES$CrAT^{M564A}$; primer CrATH343A.for (5′-GTGGGATGGTTTATGAA<u>GC</u>TGCAGCTGCAGAAGGG-3′), and primer CrATH343A.rev (5′-CCCTTCTGCAGCTGCA<u>GC</u>TTCATAAACCATCCCAC-3′) were used to construct pYES$CrAT^{H343A}$; primer CrATE347A.for (5′-GAACATGCAGCTGCAGCAGGGCCCCCCATTGTC-3′) and primer CrATE347A.rev (5′-GACAATGGGGGGCCCTGCTGCAGCTGCATGTTC-3′) were used to construct pYES$CrAT^{E347A}$; primer COTG553M.for (5′-GTTACTTACGAATTCAG<u>ATG</u>GTCGTGGTTCCCATG-3′), and primer COTG553M.rev (5′-CATGGGAACCACGAC<u>CA</u>TCTGAATTCGTAAGTAAC-3′) were used to construct pYES$COT^{G553M}$. In all the cases the mutated nucleotides are underlined. The appropriate substitutions, as well as the absence of unwanted mutations, were confirmed by sequencing the inserts.

*Expression of CrAT and COT in S. cerevisiae*—The plasmids containing wt and mutants CrAT and COT were expressed in yeast cells, and mitochondrial and peroxisomal cell extracts were prepared as previously described (18, 19). A strain of *S. cerevisiae* devoid of COT activity and lacking the endogenous *CAT2* gene (FY23Δ*cat2* (*MATa trp1 ura3* Δ*cat2*::*LEU2*)) was used as an expression system. Although this strain conserves two additional CrAT genes (*YAT1* and *YAT2*) (30), its carnitine acetyltransferase activity in the conditions in which it was expressed was not detected.

*Expression and Purification of Rat CrAT Wild-type in E. coli*—For expression and purification of rat CrAT protein the glutathione *S*-transferase (GST) gene fusion system (Amersham Biosciences) was used. The construction pGEX-$CrAT^{wt}$ was transformed into *E. coli* BL21, and fusion protein GST-CrAT was overexpressed overnight after the addition of 0.1 mM isopropyl-1-thio-β-D-galactopyranoside at 18 °C. The soluble fusion protein was purified from bacterial lysates using glutathione-Sepharose 4B with a batch method. Finally, CrAT was eluted by cleavage of the fusion protein with the site-specific protease PreScission protease (Amersham Biosciences). Purity of rat CrAT protein was checked by SDS-PAGE.

*Determination of Carnitine Acyltransferase Activity*—Carnitine acyltransferase activity was measured by a slight modification of an end

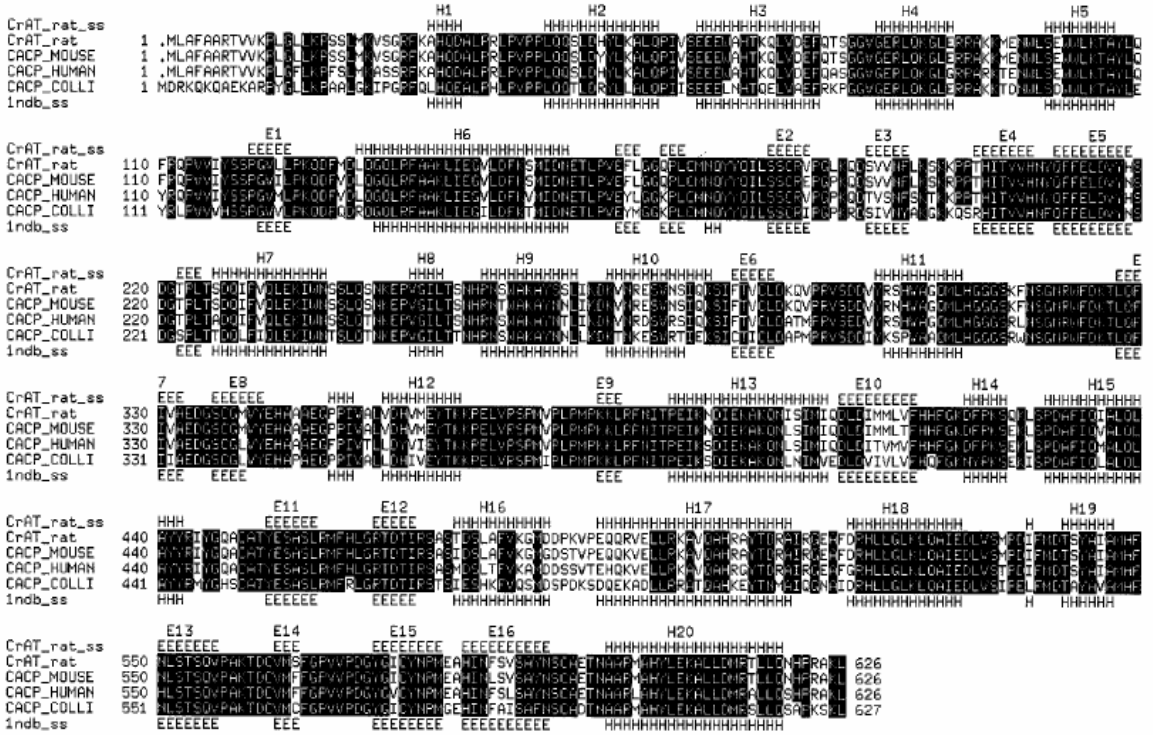

FIG. 1. **Sequence and proposed secondary structure of rat carnitine acetyltransferase (CrAT).** Alignment of amino acid sequence of carnitine acetyltransferases from rat (*CrAT-rat*), mouse (Swiss-Prot code: *CACP_MOUSE*), human (*CACP_HUMAN*), and domestic pigeon, *Columba livia* (*CACP_COLLI*). The secondary structure elements for Protein Data Bank entry 1NDB (mouse carnitine acetyltransferase) are numbered as previously published (14). The modeled secondary elements for rat CrAT are also indicated (*H*: alpha helix; *E*: beta strand). Residues are *shaded* according to conservation.

point fluorometric method (31). The assay was conducted for 8 min at 30 °C in a solution containing 0.1 mM acyl-CoA, 1.5 mM EDTA, 1.5 mM L-carnitine, 40 mM HEPES buffer (pH 7.8) in a total volume of 600 $\mu$l. Reactions were started by the addition of yeast-expressed protein: 5 $\mu$g for CrAT, 4 $\mu$g for COT, or from 0.1 to 5 $\mu$g of *E. coli*-expressed CrAT. Parallel (blank) assays were run in the absence of L-carnitine. Reactions were arrested by heat treatment (10 min at 70 °C). Proteins were sedimented by centrifugation for 10 min at 13,400 × *g*; 550 $\mu$l of the supernatant was collected, 35 $\mu$l of a stock solution (2 mg/ml) of 7-fluoro-2,1,3-benzoxadiazole-4-sulfonamide was added, and the mixture was incubated at 50 °C for 30 min. Fluorescence intensities, indicative of the binding of the CoA thiol group to 7-fluoro-2,1,3-benzoxadiazole-4-sulfonamide, were measured in 10-mm path-length glass cuvettes (700 $\mu$l) at 391 nm (excitation wavelength) and 515 nm (emission wavelength). These fluorescence intensities were compared with a standard curve for CoA between 0 and 30 nmol. All fluorometer recordings were performed with a PerkinElmer Life Sciences LS 45 luminescence spectrometer, and the enzyme activities were measured in duplicate. For determination of the $K_m$ for carnitine, acyl-CoA was fixed at 0.1 mM. For determination of the $K_m$ for acyl-CoA, carnitine concentration was fixed at 1.5 mM. Values reported are the means and standard deviations of three or four determinations. All protein concentrations were measured using the Bio-Rad protein assay with bovine albumin as standard. $K_m$ and $V_{max}$ values were calculated with the analysis of variance program.

*Generation of Anti-rat Carnitine Acetyltransferase Antibodies*—Two female New Zealand White rabbits were each injected subcutaneously on days 0, 21, 42, and 63 with 150 $\mu$g of the purified CrAT protein. The protein was emulsified 1:1 with Freund's complete adjuvant (day 0) or incomplete adjuvant (days 21, 42, and 63) in a total volume of 1 ml. Rabbits were bled completely 10 days after the third booster (day 73), and then the serum with the anti-rat CrAT antibodies was isolated. All the procedures were performed in accordance with the recommendations of the Animal Experimentation Ethical Committee of the University of Barcelona.

*Immunological Techniques*—*S. cerevisiae* protein extracts (8 $\mu$g for CrAT and 10 $\mu$g for COT) were treated with sample buffer and subjected to 8% SDS-PAGE. Electroblotting to nitrocellulose sheets was carried out for 1 h at 250 mA. Immunodetection of CrAT was performed using anti-CrAT antibodies (1:10,000 dilution), and immunodetection of COT was done with anti-COT antibodies obtained as described elsewhere (19). The blots were developed with the ECF Western blotting system from Amersham Biosciences. The quantifications were carried out using a fluorescence scanning device from Molecular Dynamics Storm 840™.

## RESULTS

*Isolation of Rat CrAT*—A cDNA fragment corresponding to rat CrAT was isolated from rat testis mRNA by RT-PCR and sequenced. The sequence has been deposited in the GenBank™ (accession no. AJ620886).

Rat CrAT mRNA encodes a predicted protein of 626 amino acids with a molecular mass of 70,800 Da (Fig. 1), which shows 96 and 90% identity with CrAT from mouse and human, respectively. The N-terminal end of the primary translation product has a sequence of 21 amino acids before the second methionine, which is the putative first amino acid in peroxisomal CrAT. By comparison with other CrATs we postulated a 29-amino acid sequence that transports the protein into mitochondria (32). Its amino acid composition is consistent with the general composition given for leader peptides that translocate cytosolic synthesized proteins into mitochondria (33).

*Re-engineering CrAT Substrate Specificity*—Inspection of the published crystal structure of CrAT revealed that acetyl-CoA points to a hydrophobic pocket at the intersection of two $\beta$-sheets (strands $\beta$1 and $\beta$8 in the N domain and strands $\beta$13 and $\beta$14 in the C domain) and helix $\alpha$12 (14). This pocket is partially occupied by the side chain of $Met^{564}$ from strand $\beta$14. Because this methionine is only present in CrAT, but not in other carnitine acyltransferases (CPT I, CPT II, or COT) (Fig. 2), in which the equivalent residue is a glycine, we hypothesized that it could play a role in the correct positioning of the

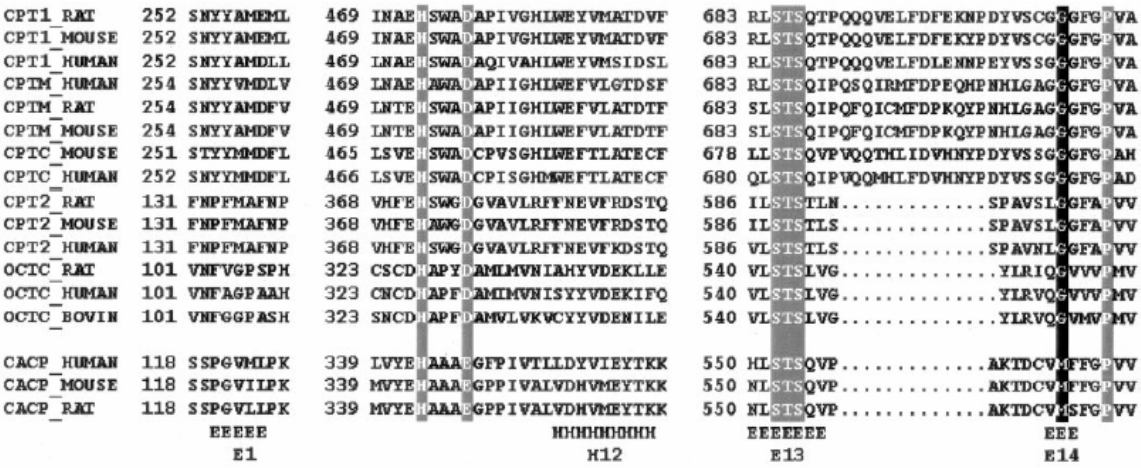


FIG. 2. **Alignment of representative sequences of mammalian carnitine-acyltransferases.** Amino acid sequence of 17 representative enzymes that catalyze short acyl-CoAs as substrates: CrAT (*CACP*) from human, mouse, and rat; and enzymes which have medium- and long-chain acyl-CoAs as substrates: L-CPT I (*CPT1*) from rat, mouse, and human; M-CPT I (*CPTM*) from human, rat, and mouse; brain CPT I (*CPTC*) from human and mouse; CPT II (*CPT2*) from rat, mouse, and human; and COT (*OCTC*) from human, rat, and bovine; were obtained from the Swiss-Prot data bank and aligned using ClustalW. The subfamily conserved residue according to acyl-CoA chain-length specificity is *shaded* in *black*: for CrAT it is a methionine; and for COT, L-CPT I, M-CPT I, brain CPT I-c, and CPT II it is a glycine. Position of catalytic histidine, catalytic aspartic/glutamic, STS catalytic domain and a conserved proline residue, are also *shaded in gray*. Secondary structure elements are indicated as in Fig. 1.

hydrocarbon chain of acyl-CoA as substrate, and therefore we prepared CrAT mutant M564G, which we then expressed in the budding yeast, *S. cerevisiae*.

Enzyme activity of yeast-expressed CrAT mutant M564G was tested for acyl-CoA substrates of various lengths and compared with wt CrAT. Wild-type CrAT was highly active toward acetyl-CoA and butyryl-CoA (Fig. 3*A*), but not toward other, longer-chain acyl-CoAs. The activity was practically zero with dodecanoyl-CoA and longer acyl-CoAs. In contrast, CrAT mutant M564G (Fig. 3*B*) was more active toward longer acyl-CoAs: it showed a new activity toward palmitoyl-CoA and a 1250-fold increase of activity toward myristoyl-CoA (Tables I and II). This figure was calculated after determination of enzyme activities with highly purified wt CrAT after expression in *E. coli* (see "Experimental Procedures"). Otherwise, activity also increased with dodecanoyl- (58-fold), decanoyl- (7-fold), octanoyl- (11-fold), and hexanoyl-CoA (7-fold), while activity toward acetyl-CoA decreased 50%. These values indicate that the long side chain of methionine impedes the positioning of medium- and long-chain acyl-CoAs in the hydrophobic pocket, but when this side chain is shortened (as in the mutant) other, longer acyl-CoAs fit the catalytic site and catalysis proceeds.

*Kinetic Characteristics of wt CrAT and Mutant M564G*—A series of kinetic experiments were performed by varying the length of the acyl-CoA substrate (from C2 to C16 acyl-CoA) with both wt CrAT and mutant M564G. The mutant showed standard saturation kinetics for both carnitine and acyl-CoA substrates, as did the wt CrAT (data not shown). This property was general for every acyl-CoA, irrespective of its length. $K_m$ values for wt CrAT varied slightly (between 23 and 33 $\mu$M) with the chain length of the substrate (Table I). $V_{max}$ was maximal for butyryl-CoA and then decreased for longer acyl-CoAs. Wild-type CrAT $V_{max}$ and catalytic efficiency (defined as $V_{max}/K_m$ ratio) for octanoyl-CoA was only 8% of those for acetyl-CoA. $K_m$ and $V_{max}$ for carnitine as substrate were also measured by varying the length of acyl-CoA. $K_m$ increased with the length of the acyl-CoA substrate. $K_m$ for carnitine with octanoyl-CoA as substrate was 5-fold that for acetyl-CoA, and concomitantly, $V_{max}$ decreased to 10% when octanoyl-CoA was the substrate in comparison with acetyl-CoA. Catalytic efficiency for carnitine also decreased; for example, catalytic efficiency for octanoyl-CoA was only 2% *versus* acetyl-CoA. This implies that short-chain acyl-CoAs are preferential substrates when the concentration of carnitine is low and that the binding of long acyl-CoAs lowers affinity for carnitine.

Different behavior was observed with CrAT mutant M564G (Table II). Although $K_m$ values for fatty acyl-CoA varied slightly with the chain length (between 11 and 32 $\mu$M), $V_{max}$ increased, particularly with hexanoyl-CoA. Another maximum of activity was also observed with myristoyl-CoA. $K_m$ for carnitine decreased when the acyl-CoA was long, showing that the mutant preferred long-chain acyl-CoAs as substrates. Catalytic efficiencies for both carnitine and acyl-CoA increased with the length of acyl-CoA, values for hexanoyl-CoA and octanoyl-CoA being the highest. In contrast to the wt CrAT, mutant M564G behaved as if its natural substrates were medium- and long-chain acyl-CoAs.

The comparison of catalytic efficiencies between octanoyl-CoA and acetyl-CoA for the wt and CrAT mutant M564G shows that this point mutation produced an increase of 103-fold. We did not compare catalytic efficiencies for longer fatty acyl-CoAs, because their activities were too low. These results were interpreted as showing that replacement of methionine by glycine increased the space for positioning of carnitine and acyl-CoA, which in turn increased the catalytic efficiency.

*Re-engineering COT Specificity*—Through the experiments performed above we had converted rat CrAT into a pseudo rat COT, which was able to catalyze medium- and long-chain acyl-CoAs. Our aim was then to achieve the opposite, that is, to transform rat COT into a pseudo rat CrAT by modifying a single amino acid. The catalytic activity of CrAT mutant M564G toward different acyl-CoAs was very similar to that of wt COT (Fig. 3, *B* and *D*). To improve our definition of the role of COT $Gly^{553}$ (orthologous to CrAT $Met^{564}$) in catalytic activity with respect to acyl-CoAs of different lengths, COT mutant G553M was prepared and expressed in *S. cerevisiae*.

Enzyme activity of yeast-expressed COT mutant G553M was tested with substrates of different length and compared with wt COT (Fig. 3). Results show that wt COT was highly active toward medium-chain acyl-CoAs: hexanoyl-, octanoyl-, and dec-

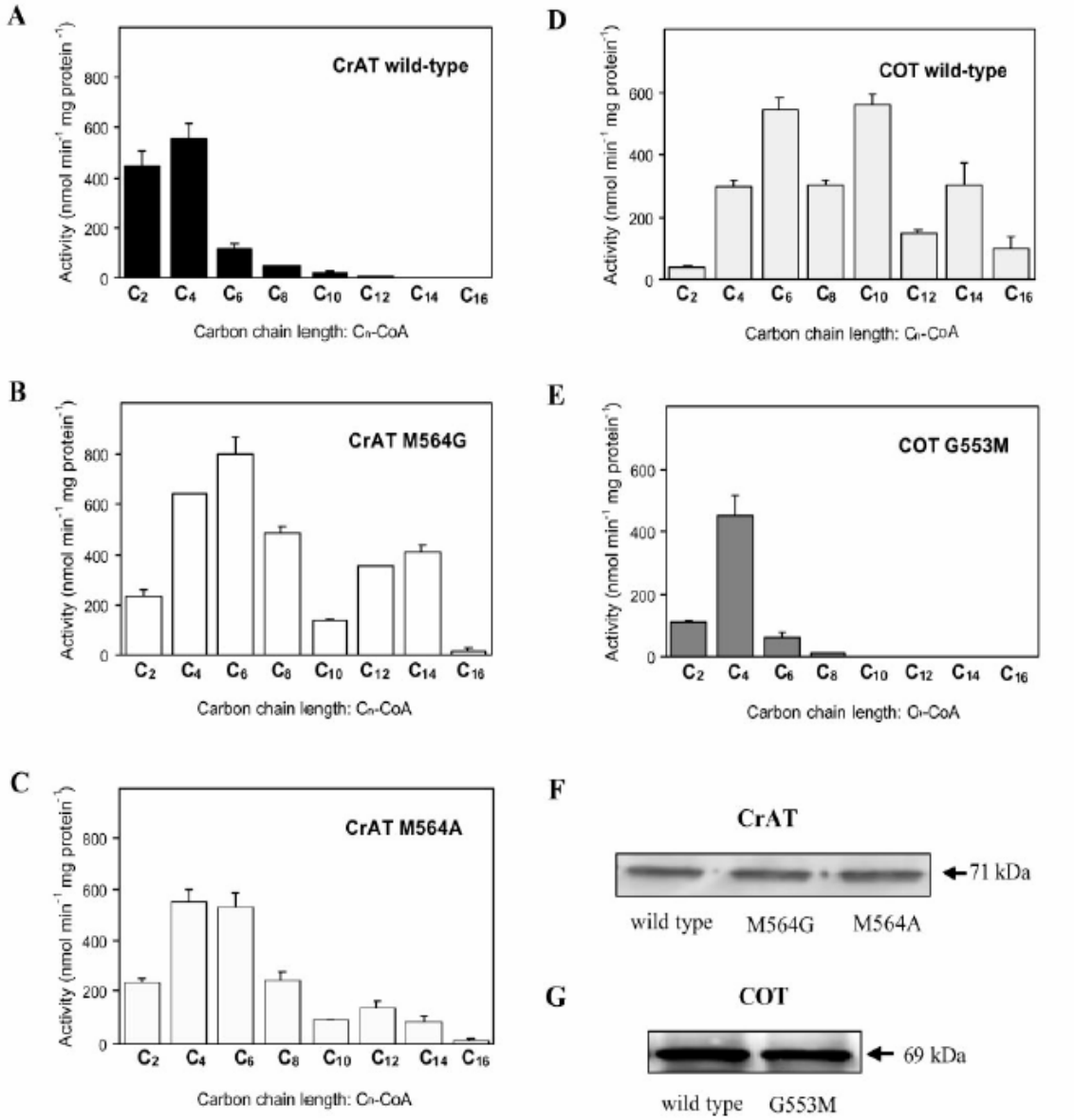


FIG. 3. **Carnitine acyltransferase activity of *S. cerevisiae* cells expressing wt CrAT and COT and the point mutants CrAT M564G, M564A, and COT G553M.** Extracts from yeast expressing wt CrAT (*A*), wt COT (*D*), and point mutants CrAT M564G (*B*), M564A (*C*), and COT G553M (*E*) were assayed for activity with acyl-CoAs of different chain length ranging from acetyl-CoA to palmitoyl-CoA, as described under "Experimental Procedures." The results are the mean ± S.D. of at least three independent experiments with different preparations. Immunoblots showing expression of wt CrAT, CrAT M564G, and M564A (*F*); and of wt COT and COT G553M (*G*). *S. cerevisiae* extracts (8 μg for CrAT and 10 μg for COT) were separated by SDS-PAGE and subjected to immunoblotting using specific antibodies. The *arrows* indicate the migration position and the molecular mass of rat CrAT (71 kDa) and rat COT (69 kDa).

anoyl-CoA, but not toward other acyl-CoAs with either a shorter or a longer hydrocarbon chain. COT mutant G553M showed much lower activity toward medium- and long-chain acyl-CoAs, but a slight increase in activity toward short-chain acyl-CoAs (acetyl-, and butyryl-CoA), showing maximum activity toward butyryl-CoA: at variance with wt COT, but the same as wt CrAT (Fig. 3).

COT mutant G553M showed a 31-fold decrease in activity when octanoyl-CoA was the substrate with respect to wt COT. Activity with hexanoyl-CoA also decreased (9-fold). Activities of COT mutant G553M toward acyl-CoAs containing between 10 and 16 carbons in their chain were undetectable, so the profile of activities toward the whole list of acyl-CoAs was practically identical to that of wt CrAT. Mutation of $Gly^{553}$ to Met in COT reproduced the substrate specificity of wt CrAT. Western blot of yeast-expressed wt and mutants CrAT and COT showed the same molecular masses and similar expression levels (Figs. 3, *F* and *G*).

*Positioning of Fatty Acyl-CoAs in the Wild-type and Mutated CrAT and COT Models*—A common model is proposed for the location of acyl-CoAs in the active center of both CrAT and COT enzymes (Fig. 4). Three-dimensional models of the rat wt CrAT and COT were generated by homology-modeling procedures using the crystallized structures of mouse and human CrAT as templates (14, 15), in a similar way to that used to construct the model for rat CPT I, as described elsewhere (34). The

TABLE I

*Enzyme activity and kinetic parameters of CrAT wt expressed in S. cerevisiae*

Mitochondrial protein from yeast expressing wt CrAT were assayed with acyl-CoAs of different carbon lengths ranging from acetyl-CoA to palmitoyl-CoA, as described under "Experimental Procedures." The results are the mean ± S.D. of at least three independent experiments with different preparations.

| Acyl-CoA | Activity | $K_m$ | | $V_{max}$ | | Catalytic efficiency | |
|---|---|---|---|---|---|---|---|
| | | Carnitine | Acyl-CoA | Carnitine | Acyl-CoA | Carnitine | Acyl-CoA |
| | *nmol·min⁻¹·mg protein⁻¹* | *μM* | | *nmol·min⁻¹·mg protein⁻¹* | | $V_{max}/K_m$ | |
| $C_2$-CoA | 442 ± 66 | 203 ± 21 | 22.8 ± 1.0 | 515 ± 56 | 550 ± 99 | 2.53 | 24.1 |
| $C_4$-CoA | 553 ± 62 | 220 ± 54 | 30.7 ± 2.8 | 567 ± 97 | 685 ± 85 | 2.58 | 22.3 |
| $C_6$-CoA | 119 ± 16 | 567 ± 80 | 33.2 ± 4.6 | 176 ± 22 | 148 ± 5.1 | 0.31 | 4.46 |
| $C_8$-CoA | 45.7 ± 6.5 | 964 ± 120 | 24.7 ± 6.5 | 53 ± 8.0 | 45.0 ± 7.1 | 0.05 | 1.82 |
| $C_{10}$-CoA | 20.3 ± 4.1 | ND[a] | ND | ND | ND | ND | ND |
| $C_{12}$-CoA | 6.0 ± 2.6 | ND | ND | ND | ND | ND | ND |
| $C_{14}$-CoA | 0.33 ± 0.07[b] | | | | | | |
| $C_{16}$-CoA | UD[c] | | | | | | |

[a] ND, not determined.
[b] This activity was obtained using purified rat CrAT expressed in *E. coli*.
[c] UD, undetectable activity.

TABLE II

*Enzyme activity and kinetic parameters of CrAT mutant M564G in S. cerevisiae*

Mitochondrial protein from yeast expressing CrAT mutant M564G were assayed with acyl-CoAs of different carbon length ranging from acetyl-CoA to palmitoyl-CoA, as described under "Experimental Procedures." The results are the mean ± S.D. of at least three independent experiments with different preparations.

| Acyl-CoA | Activity | $K_m$ | | $V_{max}$ | | Catalytic efficiency | |
|---|---|---|---|---|---|---|---|
| | | Carnitine | Acyl-CoA | Carnitine | Acyl-CoA | Carnitine | Acyl-CoA |
| | *nmol·min⁻¹·mg protein⁻¹* | *μM* | | *nmol·min⁻¹·mg protein⁻¹* | | $V_{max}/K_m$ | |
| $C_2$-CoA | 234 ± 30 | 339 ± 44 | 31.7 ± 5.3 | 197 ± 20.8 | 243 ± 25 | 0.58 | 7.7 |
| $C_4$-CoA | 641 ± 3.2 | 170 ± 45 | 14.8 ± 1.0 | 742 ± 133 | 872 ± 125 | 4.4 | 59 |
| $C_6$-CoA | 802 ± 66 | 164 ± 11 | 22.3 ± 6.0 | 1145 ± 255 | 1120 ± 106 | 7.0 | 50 |
| $C_8$-CoA | 488 ± 24 | 86.0 ± 6.1 | 10.9 ± 3.6 | 522 ± 106 | 653 ± 110 | 6.1 | 60 |
| $C_{10}$-CoA | 136 ± 7.3 | 26.9 ± 6.9 | 10.8 ± 1.7 | 153 ± 10.6 | 257 ± 41.6 | 5.7 | 24 |
| $C_{12}$-CoA | 350 ± 0.5 | ND[a] | ND | ND | ND | ND | ND |
| $C_{14}$-CoA | 409 ± 29 | 309 ± 50 | 12.7 ± 2.5 | 562 ± 84.6 | 505 ± 83.5 | 1.9 | 40 |
| $C_{16}$-CoA | 18.1 ± 5.9 | ND | ND | ND | ND | ND | ND |

[a] ND, not determined.

models for the mutants CrAT M564G and COT G553M were built using the structural models of their respective wt enzymes as templates to ensure minimal variation in the atomic position of the residues located close to the active center of both proteins. The carnitine molecule and the CoA part of the acyl-CoAs were located using the information available in the crystallized structures of mouse CrAT (PDB entries: 1NDF and 1NDI (14)). Positioning of the acyl part of the acetyl-, decanoyl-, and myristoyl-CoA substrates was modeled by the simulation docking algorithms Autodock (27, 28) and Hex (29).

The location of acetyl-CoA in the active center of the model for rat wt CrAT (Fig. 4*A*) is, as expected, very similar to that described for CoA in the crystallized mouse CrAT. The sulfur atom of the CoA molecule is close to carnitine and to the catalytic $His^{343}$, whereas the acetyl group appears to lie in a small cavity defined, by the β-sheets E1, E13, and E14, as the walls of the hollow, and by the lateral chain of residue $Met^{564}$ as the floor. Surprisingly, the shape of the cavity appears to be very different in the structure of the active center of CrAT mutant M564G (Fig. 4*B*). The small size of the side chain of $Gly^{564}$ reveals a deeper pocket in the same position as the shallow cavity in the wt molecule. This preformed pocket is now accessible to longer acyl groups, as can be modeled using myristoyl-CoA as substrate. The position of the fatty acyl part of myristoyl-CoA is very similar to that modeled for the palmitoyl part of palmitoyl-CoA in a hydrophobic pocket of CPT I (34). The open cavity of CrAT mutant M564G is surrounded by $Gly^{564}$, by hydrophobic residues $Val^{122}$, $Leu^{124}$, $Ile^{351}$, $Val^{352}$ $Val^{355}$, $Met^{359}$, $Val^{556}$, $Ala^{558}$, and $Cys^{562}$ (located in β-sheets E1, E13, and E14 and in α-helix H12, as in CPT I) and by polar residues $Asp^{356}$ and $Thr^{560}$ at the bottom. Interestingly, it appears that the cavity for longer acyl groups is preformed in CrAT and that $Met^{564}$ acts as a lid to close the access to the hydrophobic pocket (Fig. 5*A*). When the side chain of $Met^{564}$ is removed, the pocket is now accessible, extending the sensitivity of the enzyme to long-chain acyl-CoA substrates (Fig. 5*B*). This is consistent with the enzymatic activity observed when using C8, C10, C12, and C14 acyl-CoA as substrates (Fig. 3*B*).

The model for wt COT and its interaction with decanoyl-CoA is very similar to the one for CrAT mutant M564G and myristoyl-CoA. The sulfur atom of the acyl-CoA molecule is close to carnitine and to $His^{327}$, the catalytic residue, whereas the fatty acid extension is enclosed in a pocket (Fig. 4*C*) defined by the side chain of hydrophobic residues positioned in β-sheets E1, E13, and E14 and in α-helix H12: $Val^{104}$, $Ala^{332}$, $Met^{333}$, $Met^{335}$, $Val^{336}$, $Ala^{339}$, $Leu^{545}$, $Leu^{549}$, and $Ile^{551}$. The floor of the cavity is occupied by polar residues $Ser^{107}$ and $Asp^{343}$. In contrast, the structure for COT mutant G553M resembles that for wt CrAT: the side chain of $Met^{553}$ now closes the entrance to the pocket and defines a narrow cavity, structurally equivalent to that of the active center in wt CrAT, where the small acetyl group of acetyl-CoA can be fitted (Fig. 4*D*). In symmetry with CrAT, the hydrophobic cavity for long acyl-CoAs in the COT structure can be closed by the lateral chain of $Met^{553}$, which acts as a lid, like the corresponding residue in CrAT, $Met^{564}$. The model again correlates with the enzymatic activities of wt and mutant COT when using short- and long-chain acyl-CoAs as substrates (Fig. 3).

*The Mutant M564A Also Broadened the Specificity of CrAT*—Because glycine does not constrain the backbone psi/phi angles, its substitution for methionine could modify substrate specificity simply as a result of increased flexibility. To rule out this

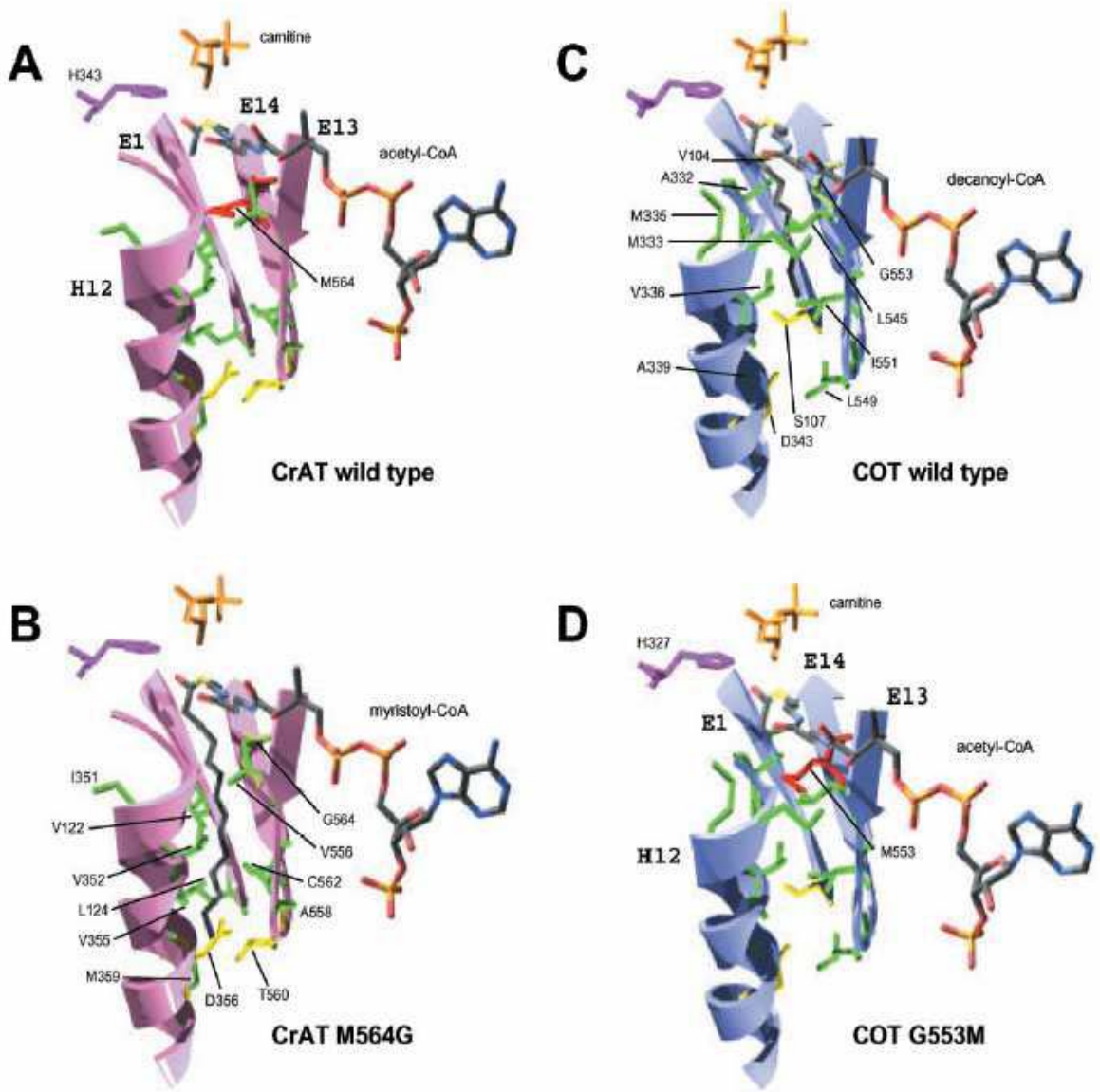


FIG. 4. **Proposed models for the positioning of fatty acyl-CoAs in the wt and mutated CrAT and COT.** *A*, location of a molecule of acetyl-CoA in the active center of wt CrAT. Position of $Met^{564}$ (*red*) as well as the secondary structure elements alpha helix 12 and beta strands 1, 13, and 14, surrounding the acetyl hollow, are indicated. The molecule of carnitine, as well as the catalytic residue $His^{343}$ are also represented. *B*, location of a molecule of myristoyl-CoA in the deep pocket opened in the CrAT mutant M564G. Positions of $Gly^{564}$, hydrophobic residues around the acyl-chain ($Val^{122}$, $Leu^{124}$, $Ile^{351}$, $Val^{352}$, $Val^{355}$, $Met^{359}$, $Val^{556}$, $Ala^{558}$, and $Cys^{562}$) and polar residues $Asp^{356}$ and $Thr^{560}$ are indicated. *C*, a molecule of decanoyl-CoA in the hydrophobic pocket defined by alpha helix 12 and beta strands 1, 13, and 14 of wt COT. Positions of $Val^{104}$, $Ala^{332}$, $Met^{333}$, $Met^{335}$, $Val^{336}$, $Ala^{339}$, $Leu^{545}$, $Leu^{549}$, and $Ile^{551}$ and the polar residues $Ser^{107}$ and $Asp^{343}$ are indicated. *D*, model for the location of a molecule of acetyl-CoA in the shallow cavity closed by $Met^{553}$ (*red*) of COT mutant G553M. Carnitine, $His^{327}$, and the positions of secondary structure elements helix 12 and beta strands 1, 13, and 14 are also represented.

possibility, we prepared another CrAT mutant, M564A. Alanine is also a small amino acid, but, unlike glycine, it does not affect flexibility. So if methionine/glycine acts as a molecular gate to prevent/permit acyl-CoA binding as a function of chain length, the alanine mutant should behave similarly to the glycine. The change of specificity of the alanine mutant might not be as pronounced, but it would still be able to catalyze acyl-CoAs longer than acetyl-CoA and butyryl-CoA.

Accordingly, we expressed the CrAT mutant M564A in *S. cerevisiae*, and the extracts were assayed for carnitine acyltransferase activity using acyl-CoAs of various chain lengths as substrates. The results were similar to those found in mutant M564G, (Fig. 3*C*). For instance, CrAT mutant M564A activity toward myristoyl-CoA increased 242-fold with respect to the wt CrAT. The -fold activation of the M564A mutant toward acyl-CoAs of between C6 and C12 ranged between 5- and 23-fold. CrAT M564A also showed some activity toward palmitoyl-CoA (11 $nmol \cdot min^{-1} \cdot mg\ protein^{-1}$), which was absent in wt CrAT. In addition, the activity of CrAT mutant M564A toward its natural substrate acetyl-CoA was less than half that of wt CrAT.

*Activity of CrAT Mutants H343A and E347A*—It is generally accepted that a histidine is the main catalytic residue in carnitine acyltransferases. This critical histidine residue had been mutated in several proteins of the carnitine acyltransferase family like rat CPT II (16), rat L-CPT-I (18), rat COT (19), and

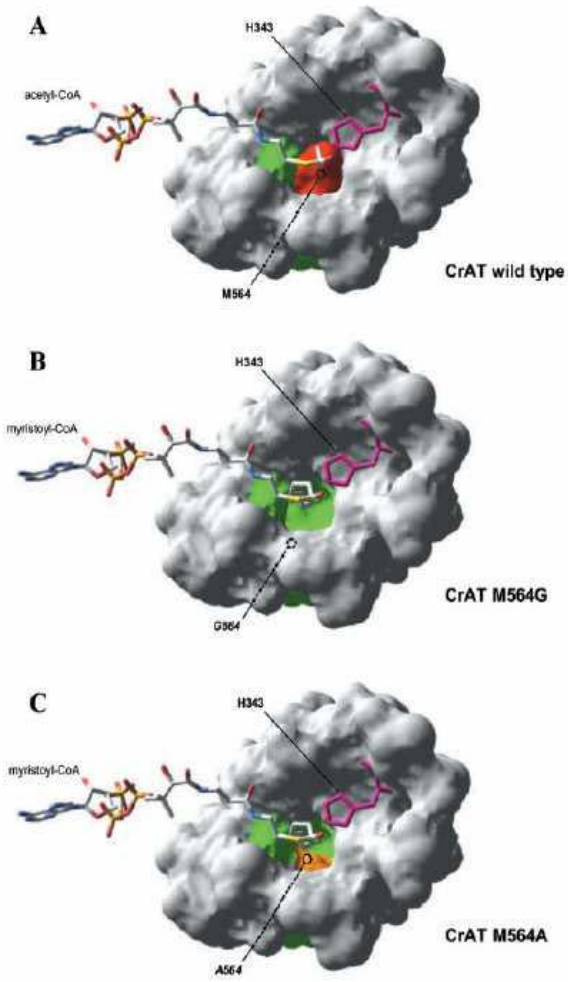


FIG. 5. **Substrate docking in wt CrAT and mutants.** Proposed location of acetyl-CoA and myristoyl-CoA acyl-chains in the active centers of rat CrAT wt (*A*), mutant M564G (*B*), and mutant M564A (*C*) surface structural models, respectively. Hydrophobic residues in the walls of the deep pocket are colored in *green*. $Met^{564}$ surface, closing the cavity in wild-type CrAT, is depicted in *red*. $Ala^{564}$ is depicted in *yellow*. Catalytic $His^{343}$ is also represented (*pink trace*).

human peroxisomal CrAT (15), and in all cases the mutation completely abolished enzyme activity. To see whether the homologous histidine behaved similarly in rat CrAT, we mutated CrAT $His^{343}$ to Ala, because this position is orthologous to other carnitine acyltransferases. Enzyme activity of CrAT mutant H343A was abolished.

We also mutated $Glu^{347}$ to Ala in rat CrAT. In almost all the other members of the family, an aspartate is found at this position, which could functionally be substituted for glutamate. The mutation of the $Glu^{347}$ to Ala resulted in total loss of catalytic activity.

Both CrAT mutants H343A and E347A were expressed in *S. cerevisiae* at similar levels to the wt (data not shown), on the basis of which the hypothesis that the abolition of activity was caused by low protein expression was ruled out.

## DISCUSSION

Previous to this study, an mRNA sequence of rat CrAT had been reported, based on the *in silico* localization of several open reading frames (accession number XM_242301) observed in the genomic rat CrAT sequence (accession number NW_047651). The genomic organization of the postulated rat CrAT was similar to CrATs from various organisms (35). However, it was also postulated to contain an extra exon (exon 7bis) not found in any other organism, solely on the basis of the observation of an open reading frame of 81 nt within intron 7. Our findings after sequencing the rat CrAT cDNA did not reveal the proposed exon 7bis. To establish whether this exon is present in mature CrAT mRNA, a shorter cDNA fragment comprising the putative exon 7bis was PCR-amplified. No such sequence was found, from which it was concluded that rat CrAT does not contain an exon 7bis. Nor was such an exon observed in any published CrAT cDNA sequence or in 40 published expressed sequence tag sequences from rat CrAT, and no such amino acid sequence can be aligned with protein sequences of CPT I, CPT II, or COT from various organisms. Alternatively, if such an exon were to exist, rat testis expression of the processed mRNA containing exon 7bis would be undetectable even using PCR amplification.

The use of a mutant strain of *S. cerevisiae* devoid of CrAT and COT activity allowed us to express wt and mutant rat CrAT and COT cDNAs and study their kinetic characteristics. The results show that the yeast-expressed CrAT behaves like rat CrAT from mitochondria (36). This is the first time that mammalian CrAT has been expressed in yeast.

The carnitine acyltransferases family has a common catalytic mechanism, which is the transfer of the fatty acid moiety from fatty acyl-CoA to carnitine in a process that involves deprotonation of carnitine and nucleophilic attack of the carbonyl carbon of the thioester bond of acyl-CoA. In CrAT the residue implicated in this process is $His^{343}$. Mutant H343A was expressed in *S. cerevisiae*, and the activity of the mutant was abolished, although the expression was practically identical to wt CrAT. Other carnitine acyltransferases stabilize the catalytic histidine through an aspartic acid. $Glu^{347}$ occupies the same position in CrAT as an aspartic residue in other carnitine acyltransferases (34). The important role of $Glu^{347}$ in CrAT activity is clearly defined, because mutant E347A abolished enzyme activity, as seen in CPT II (16).

This general mechanism, which also corresponds to a similar three-dimensional structure (34), is nevertheless complemented by substrate-specific characteristics. Substrate specificity is now well defined, on the basis of the studies of various groups: CrAT catalyzes short-chain acyl-CoAs (acetyl-CoA, propionyl-CoA, and butyryl-CoA) (36–39), whereas COT catalyzes medium-chain acyl-CoAs containing between 6 and 12 carbons (40, 41), and CPT I and CPT II catalyze palmitoyl-CoA and long-chain fatty acyl-CoAs (40). We hypothesized that a structural feature on the enzyme might be responsible for substrate specificity, depending the length of the acyl-CoAs. We addressed this question with CrAT and COT.

The putative amino acid residue responsible for governing the access of the acyl-CoA was identified by close examination of the catalytic site in CrAT crystals. The recent report of the crystal structure of mouse (14) and human CrAT (15) suggested $Met^{564}$ as a candidate, because its side chain is voluminous and projects into the putative cavity where the acyl-CoA may enter. The fact that methionine is a bulky residue suggests a possible role in permitting the access of only short-chain substrates such as acetyl-CoA and butyryl-CoA. Interestingly, according to the information gleaned from multiple alignment of the sequences of the carnitine acyltransferases family of proteins, the presence of either a Gly or a Met residue in the same position is, respectively, a common feature in all long-chain and short-chain acyl-CoA enzymes. This type of position, in multiple alignment with a pattern of variation related to differences in function of the corresponding groups of subfamilies of pro-

teins, implies functional and structural changes that are selected through evolution. Such residues are conceptually related with specific active sites, substrate binding sites, or inhibitor interaction patches (42), as demonstrated in the case of the interaction of several members of the carnitine acyltransferases family with the inhibitor malonyl-CoA (43).

*Mutation of Met$^{564}$ to Glycine Opens the Hydrophobic Pocket to Medium- and Long-chain Acyl-CoAs*—By alignment we identified the orthologous amino acid Met$^{564}$ residue in carnitine acyltransferases that catalyze substrates of longer chain than acetyl-CoA. It was clear that not only COT but also CPT I and CPT II contain a glycine in this position (Fig. 2). This suggested that the smaller glycine was probably the residue that allows free access of the long-chain fatty acyl-CoAs, whereas the larger side chain of Met$^{564}$ prevented the access of long-chain acyl-CoAs. CrAT mutant M564G produced positive results that vindicate these expectations.

The increases in activity and catalytic efficiency toward long-chain acyl-CoAs in the CrAT mutant M564G were not accompanied by changes in $K_m$ for acyl-CoA. Maximal changes were observed in $V_{max}$ and catalytic efficiency, which suggests that these increases in catalytic activity are attributable to the altered accessibility of the catalytic site.

The Michaelis constants for substrates ranging from acetyl-CoA to octanoyl-CoA are very similar (Table I). This poses the question as to whether the various acyl-CoAs in the wt model are located in the hydrophobic pocket or in the catalytic channel. If the latter were the case, acyl-CoAs would displace carnitine from its site. This appears to occur, as carnitine $K_m$ increases when the chain length of acyl-CoA increases. Carnitine is presumably displaced, and catalysis is prevented, as indicated by the low $V_{max}$ of the wt CrAT in the presence of long-chain acyl-CoAs. If the hydrophobic pocket is open, as shown in the CrAT mutant M564G, the long hydrocarbon chain can occupy it. Consequently, carnitine $K_m$ decreases when long-chain acyl-CoAs increase (except for myristoyl-CoA) and catalytic efficiencies for medium and long-chain acyl-CoA increase, and catalysis proceeds.

*Mutation of COT Gly$^{553}$ to Methionine Closes the Hydrophobic Pocket*—These hypotheses were confirmed by the reverse experiment: we mutated COT Gly$^{553}$ to methionine, and the new mutant behaved like wt CrAT. Results of COT mutant G553M activity in relation with the acyl-CoA used as substrate are very similar to those of wt CrAT. The same applies to CrAT mutant M564G and wt COT: the pattern of activities in relation to acyl-CoAs of different lengths is very similar. In both cases the enzymes containing glycine rather than methionine (CrAT mutant M564G and wt COT) present high enzyme activities with medium and long chain fatty acyl-CoAs, whereas their activity toward acetyl-CoA is low.

An alternative explanation to the model of methionine/glycine acting as a gate to permit the location of longer acyl-CoAs could be based on increased flexibility of the mutant form, because glycine does not constrain the backbone psi/phi angles. Methionine, a larger residue, would render a more rigid environment, which would limit substrate binding. To discern between these two models, an intermediate situation was tested in which the Met$^{564}$ residue in CrAT was substituted by alanine (Fig. 5*C*). The presence of a methyl group in the side chain of alanine would mimic the presence of the methionine in terms of backbone flexibility (reducing the degrees of freedom of the phi/psi angles of the backbone), but, in contrast, it would also reflect the small size of the glycine residue. The results obtained in these new conditions, which were similar to those obtained in the Gly mutant, strongly support the gate model. This can be taken as a demonstration that a single mutant is able to switch the substrate specificity of CrAT and COT. Kinetic data together with information obtained from the three-dimensional models of wt or CrAT and COT mutants indicate that CrAT Met$^{564}$ and its orthologous COT Gly$^{553}$ are the residues responsible for the substrate specificity of these enzymes.

Wild type CrAT and COT have 32% amino acid sequence identity and, accordingly, the pattern of activity of the two enzymes toward acyl-CoAs of various lengths is very different. It is noteworthy that CrAT mutant M564G retains the same sequence identity with wt COT; however, the substrate specificity of this mutant is practically identical to that of wt COT. The same argument applies to COT; COT mutant G553M shares 32% identity with wt CrAT; however, its substrate specificity is practically identical to wt CrAT. These figures confirm that Met$^{564}$ is the amino acid responsible for the acyl-CoA specificity. Despite the fact that 68% of the amino acids are different in mutant CrAT and wt COT, the change of only one critical amino acid has rendered both proteins practically identical in terms of substrate specificity.

To our knowledge, this is the first study to show that mutation of a single amino acid leads to such dramatic modification of specificity in the various enzymes that use acyl-CoAs of various lengths. Studies carried out in acyl-CoA dehydrogenase (44, 45) show that a small change in specificity is obtained after mutation of three residues or more. Mutation of one residue slightly modified substrate specificity in the hydrolysis of esters from *Burkholderia cepacia*, and the combined action of two mutations increased the specificity to *p*-nitrophenyl palmitate by about 5-fold (46). Analogous results were obtained with *Candida rugosa* lipase, in which mutation L304F led to a 3-fold increase in the hydrolysis of a randomized oil *versus* wt enzyme (47).

The hydrophobic pocket of CrAT described in this study is the same as the one we proposed for CPT I (34). In that case, the orthologous glycine, which allows correct positioning of acyl-CoA, is surrounded by two other glycines conforming a gap that is wide enough to allow the entry of the hydrocarbon chain into the cavity before catalysis.

In summary, for the first time we have identified an amino acid residue that is critical to fatty acyl chain-length specificity in CrAT. This study may enhance our understanding of the structure-function relationship for other carnitine acyltransferases within the context of fatty acid metabolism.

*Acknowledgment*—We thank Robin Rycroft of the Language Service for valuable assistance in the preparation of the English manuscript.

REFERENCES

1. McGarry, J. D., and Brown, N. F. (1997) *Eur. J. Biochem.* **244,** 1–14
2. Esser, V., Britton, C. H., Weis, B. C., Foster, D. W., and McGarry, J. D. (1993) *J. Biol. Chem.* **268,** 5817–5822
3. Yamazaki, N., Shinohara, Y., Shima, A., and Terada, H. (1995) *FEBS Lett.* **363,** 41–45
4. Price, N. T., van der Leij, F. R., Jackson, V. N., Corstorphine, C. G., Thomson, R., Sorensen, A., and Zammit, V. A. (2002) *Genomics* **80,** 433–442
5. Bieber, L. L., Krahling, J. B., Clarke, P. R., Valkner, K. J., and Tolbert, N. E. (1981) *Arch. Biochem. Biophys.* **211,** 599–604
6. Bieber, L. L. (1988) *Annu. Rev. Biochem.* **57,** 261–283
7. Zammit, V. A. (1999) *Prog. Lipid. Res.* **38,** 199–224
8. Brunner, S., Kramar, K., Denhardt, D. T., and Hofbauer, R. (1997) *Biochem. J.* **322,** 403–410
9. Kalaria, R. N., and Harik, S. I. (1992) *Ann. Neurol.* **32,** 583–586
10. Makar, T. K., Cooper, A. J., Tofel-Grehl, B., Thaler, H. T., and Blass, J. P. (1995) *Neurochem. Res.* **20,** 705–711
11. DiDonato, S., Rimoldi, M., Moise, A., Bertagnoglio, B., and Uziel, G. (1979) *Neurology* **29,** 1578–1583
12. Brevetti, G., Angelini, C., Rosa, M., Carrozzo, R., Perna, S., Corsi, M., Matarazzo, A., and Marcialis, A. (1991) *Circulation* **84,** 1490–1495
13. Melegh, B., Seress, L., Bedekovics, T., Kispal, G., Sümegi, B., Trombitas, K., and Mehes, K. (1999) *J. Inher. Metab. Dis.* **22,** 827–838
14. Jogl, G., and Tong, L. (2003) *Cell* **112,** 113–122
15. Wu, D., Govindasamy, L., Lian, W., Gu, Y., Kukar, T., Agbandje-McKenna, M., and McKenna, R. (2003) *J. Biol. Chem.* **278,** 13159–13165
16. Brown, N. F., Anderson, R. C., Caplan, S. L., Foster, D. W., and McGarry, J. D.

(1994) *J. Biol. Chem.* **269,** 19157–19162
17. Govindasamy, L., Kukar, T., Lian, W., Pedersen, B., Gu, Y., Agbandje-McKenna, M., Jin, S., McKenna, R., and Wu, D. (2004) *J. Struct. Biol.* **146,** 416–424
18. Morillas, M., Gómez-Puertas, P., Roca, R., Serra, D., Asins, G., Valencia, A., and Hegardt, F. G. (2001) *J. Biol. Chem.* **276,** 45001–45008
19. Morillas, M., Clotet, J., Rubí, B., Serra, D., Asins, G., Ariño, J., and Hegardt, F. G. (2000) *FEBS Lett.* **466,** 183–186
20. Guex, N., and Peitsch, M. C. (1997) *Electrophoresis* **18,** 2714–2723
21. Guex, N., Diemand, A., and Peitsch, M. C. (1999) *Trends. Biochem. Sci.* **24,** 364–367
22. Peitsch, M. C. (1995) *Bio/Technology* **13,** 658–660
23. Peitsch, M. C. (1996) *Biochem. Soc. Trans.* **24,** 274–279
24. Hooft, R. W.W., Vriend, G., Sander, C., and Abola, E. E. (1996) *Nature* **381,** 272
25. Vriend, G. (1990) *J. Mol. Graph.* **8,** 52–56
26. Laskowski, R. A., MacArthur, M. W., Moss, D. S., and Thornton, J. M. (1993) *J. Appl. Cryst.* **26,** 283–291
27. Goodsell, D. S., Morris, G. M., and Olson, A. J. (1996) *J. Mol. Recognit.* **9,** 1–5
28. Morris, G. M., Goodsell, D. S., Halliday, R. S., Huey, R., Hart, E., Belew, R. K., and Olson, A. J. (1998) *J. Comput. Chem.* **19,** 1639–1662
29. Ritchie, D. W., and Kemp, G. J. (2000) *Proteins* **39,** 178–194
30. Swiegers, J. H., Dippenaar, N., Pretorius, I. S., and Bauer, F. F. (2001) *Yeast* **18,** 585–595
31. Hassett, R. P., Crockett, E. L. (2000) *Anal. Biochem.* **287,** 176–179
32. Corti, O., DiDonato, S., and Finocchiaro, G. (1994) *Biochem. J.* **303,** 37–41
33. Von Heijne, G. (1986) *EMBO J.* **5,** 1335–1342
34. Morillas, M., López-Viñas, E., Valencia, A., Serra, D., Gómez-Puertas, P., Hegardt, F. G., and Asins, G. (2004) *Biochem. J.* **379,** 777–784
35. van der Leij, F. R., Huijkman, N. C. A., Boomsma, C., Kuipers, J. R. G., and Bartelds, B. (2000) *Mol. Genet. Metab.* **71,** 139–153
36. Miyazawa, S., Ozasa, H., Furuta, S., Osumi, T., and Hashimoto, T. (1983) *J. Biochem.* **93,** 439–451
37. Chase, J. F. A. (1967) *Biochem. J.* **104,** 510–518
38. Bloisi, W., Colombo, I., Garavaglia, B., Giardini, R., Finocchiaro, G., and Didonato, S. (1990) *Eur. J. Biochem.* **189,** 539–546
39. Colucci, W. J., Gandour, R. D. (1988) *Bioorganic. Chem.* **16,** 307–334
40. Miyazawa, S., Ozasa, H., Osumi, T., and Hashimoto, T. (1983) *J. Biochem.* **94,** 529–542
41. Farrell, S. O., Fiol, C. J., Reddy, J. K., and Bieber, L. L. (1984) *J. Biol. Chem.* **259,** 13089–13095
42. López-Romero, P., Gómez, M. J., Gómez-Puertas, P., and Valencia, A. (2004) in *Principles and Practice. Methods in Proteome and Protein Analysis* (Kamp, R. M., Calvete, J., and Choli-Papadopoulou, T., eds) pp. 62–82, Springer-Verlag, Berlin
43. Morillas, M., Gómez-Puertas, P., Bentebibel, A., Selles, E., Casals, N., Valencia, A., Hegardt, F. G., Asins, G., and Serra, D. (2003) *J. Biol. Chem.* **278,** 9058–9063
44. He, M., Burghardt, T. P., and Vockley, J. (2003) *J. Btol. Chem.* **278,** 37974–37986
45. Souri, M., Aoyama, T., Yamaguchi, S., and Hashimoto, T. (1998) *Eur. J. Biochem.* **257,** 592–598
46. Yang, J., Koga, Y., Nakano, H., and Yamane, T. (2002) *Prot. Eng. Des. Sel.* **15,** 147–152
47. Schmitt, J., Brocca, S., Schmid, R. D., and Pleiss, J. (2002) *Prot. Eng. Des. Sel.* **15,** 595–601

# Mutagenesis of Specific Amino Acids Converts Carnitine Acetyltransferase into Carnitine Palmitoyltransferase†

Antonio G. Cordente,‡ Eduardo López-Viñas,§ María Irene Vázquez,‡ Paulino Gómez-Puertas,§ Guillermina Asins,‡ Dolors Serra,‡ and Fausto G. Hegardt*,‡

*Department of Biochemistry and Molecular Biology, School of Pharmacy, University of Barcelona, E-08028 Spain, and Centro de Biologia Molecular "Severo Ochoa", Consejo Superior de Investigaciones Cientificas, Cantoblanco, E-28049 Madrid, Spain*

*Received February 8, 2006; Revised Manuscript Received March 22, 2006*

ABSTRACT: Carnitine acyltransferases catalyze the exchange of acyl groups between carnitine and CoA. The members of the family can be classified on the basis of their acyl-CoA selectivity. Carnitine acetyltransferases (CrATs) are very active toward short-chain acyl-CoAs but not toward medium- or long-chain acyl-CoAs. Previously, we identified an amino acid residue ($Met^{564}$ in rat CrAT) that was critical to fatty acyl-chain-length specificity. M564G-mutated CrAT behaved as if its natural substrates were medium-chain acyl-CoAs, similar to that of carnitine octanoyltransferase (COT). To extend the specificity of rat CrAT to other substrates, we have performed new mutations. Using in silico molecular modeling procedures, we have now identified a second putative amino acid involved in acyl-CoA specificity ($Asp^{356}$ in rat CrAT). The double CrAT mutant D356A/M564G showed 6-fold higher activity toward palmitoyl-CoA than that of the single CrAT mutant M564G and a new activity toward stearoyl-CoA. We show that by performing two amino acid replacements a CrAT can be converted into a pseudo carnitine palmitoyltransferase (CPT) in terms of substrate specificity. To change CrAT specificity from carnitine to choline, we also prepared a mutant CrAT that incorporates four amino acid substitutions (A106M/T465V/T467N/R518N). The quadruple mutant shifted the catalytic discrimination between L-carnitine and choline in favor of the latter substrate and showed a 9-fold increase in catalytic efficiency toward choline compared with that of the wild-type. Molecular in silico docking supports kinetic data for the positioning of substrates in the catalytic site of CrAT mutants.

Carnitine acyltransferases catalyze the exchange of acyl groups between carnitine and CoA, and play a central role in fatty acid metabolism in eukaryotes. There are three carnitine acyltransferase families that differ in their acyl-chain-length selectivity: carnitine palmitoyltransferases (CPTs[1]), CPT I, and CPT II catalyze long-chain fatty acids, and carnitine octanoyltransferase (COT) prefers medium-chain fatty acids, whereas carnitine acetyltransferase (CrAT) uses short-chain acyl-CoAs (*1*, *2*).

CPT I and CPT II are essential for mitochondrial $\beta$-oxidation and are located in the outer and inner mitochondrial membranes, respectively, facilitating the transfer of long-chain fatty acids from the cytoplasm to the mitochondrial matrix. CPT I is the rate-limiting step in $\beta$-oxidation (*3*). COT is localized in peroxisomes and mediates the transport of medium-chain fatty acids from peroxisomes to mitochondria through the conversion of acyl-CoAs, shortened by peroxisomal $\beta$-oxidation, into acyl-carnitine (*4*). CrAT catalyzes the reversible conversion of acetyl-CoA and carnitine to acetylcarnitine and free CoA.

Because of the impermeability of organelle membranes to CoA, CrATs function in a compartmental buffering system by maintaining the appropriate levels of acetyl-CoA and CoA in cellular compartments. Mitochondrial CrAT plays a major role in modulating matrix acetyl-CoA concentration. The production and utilization of acetyl-CoA in the mitochondrial matrix occurs at a major metabolic crossroad. The regulation of the fate of acetyl-CoA is mediated, to a large extent, by the effects of the molecule itself on pyruvate dehydrogenase kinase, which is inhibited by a high acetyl-CoA/CoA ratio. In the liver, mitochondrial acetyl-CoA also activates the key gluconeogenic enzyme pyruvate carboxylase. Therefore, high rates of $\beta$-oxidation of fatty acids result in the activation of gluconeogenesis from pyruvate and its precursors (*5*). In mammalian tissues, CrATs can also contribute to the excretion of excess or harmful acyl molecules as acylcarnitines (*6*). CrATs also appear to play an important role in human health. For example, decreases in CrAT activity have been reported in patients with disorders of the nervous system, such as Alzheimer's disease (*7*), ataxic encephalopathy (*8*), and several vascular diseases (*9*, *10*). Moreover, it has been recently reported that hepatic overexpression of

† This study was supported by Grants SAF 2004-06843-C03-01/03 from the Dirección General de Investigación Científica y Técnica, by grant C3/08 from the Fondo de Investigación Sanitaria of the Instituto de Salud Carlos III, Red de Centros RCMN from the Ministerio de Sanidad y Consumo, Madrid, Spain, and by a grant from the Fundación Ramón Areces. A.G.C, E.L.-V., and M.I.V. were recipients of fellowships from the Ministerio de Ciencia y Tecnologia, the Fundación Ramón Areces, and Generalitat de Catalunya, respectively.

* To whom correspondence should be addressed. Phone: +34 93 4024523. Fax: +34 93 4024520. E-mail: fgarciaheg@ub.edu and dserra@ub.edu.

‡ University of Barcelona.

§ Consejo Superior de Investigaciones Cientificas.

[1] Abbreviations: CrAT, carnitine acetyltransferase; COT, carnitine octanoyltransferase; CPT, carnitine palmitoyltransferase; ChAT, choline acetyltransferase; wt, wild-type; 3-D, three-dimensional.

10.1021/bi0602664 CCC: $33.50 
Published on Web 04/25/2006 PAGE EST: 8.1

malonyl-CoA decarboxylase reverted muscle, liver, and whole-animal insulin resistance (*11*). These findings were accompanied by a marked decrease in $\beta$-hydroxybutyryl-carnitine in muscle samples. This was interpreted as an indication that an improvement of the mitochondrial function of insulin-resistant muscle impedes the accumulation of acetyl-CoA, thereby preventing ketogenesis. In these conditions, carnitine acetyltransferase can be critical because of its buffering action in maintaining the appropriate levels of acetyl-CoA and CoA.

The crystal structures of the mouse and human CrAT have been reported alone and in complex with their substrates carnitine or CoA (*12*, *13*). The CrAT structure contains two domains that share the same backbone fold. The active site is located at the interface of the two domains, and carnitine and CoA are bound in a tunnel on opposite sides of the catalytic histidine residue. More recently, the 3-D structure of mouse COT (*14*) was reported, alone and in complex with the substrate octanoylcarnitine, showing for the first time, the structure of the acyl moiety binding site in the carnitine acyltransferase family. The overall structure of COT is very similar to that of CrAT, although there are significant differences in the acyl group binding region, which are responsible for the differing substrate specificities of the two enzymes.

We and others recently reported that a single amino acid determined the acyl-CoA substrate specificity of CrAT and COT ($Met^{564}$ and $Gly^{553}$, respectively) (*14*−*16*). We demonstrated, by kinetic experiments and 3-D models in rat CrAT, that the mutation of this voluminous methionine to the smaller glycine (CrAT M564G mutant) permits the access of medium-chain acyl-CoAs to the hydrophobic pocket (*15*). Data from the mouse CrAT M564G mutant crystal confirm our hypothesis because they reveal a deep acyl group binding pocket that can accommodate medium-chain acyl-CoAs (*16*). Surprisingly, rat CrAT mutant M564G was very active toward myristoyl-CoA but much less so toward palmitoyl-CoA, suggesting that other amino acids may be responsible for governing the access of acyl-CoAs longer than myristoyl-CoA.

Choline acetyltransferase (ChAT) belongs to the choline/carnitine acyltransferase family and catalyzes a reaction similar to that of CrAT except that the acetyl group from acetyl-CoA is transferred to choline instead of carnitine. The difference between these two substrates is that carnitine has an additional carboxymethyl group that replaces a hydrogen at $C_1$ of the choline. The recent publication of the rat ChAT crystal (*17*, *18*) and several mutagenesis studies (*19*−*21*) have led to a model for choline/carnitine discrimination in ChAT on the basis of both electrostatic and steric factors. In the former, two of the residues that play critical roles in rat CrAT by electrostatically interacting with the carboxylate group of carnitine, $Thr^{465}$, and $Arg^{518}$ are replaced by neutral amino acids ($Val^{459}$ and $Asn^{514}$) in rat ChAT. Both residues were mutated by Cronin (*19*) in rat ChAT to their counterparts in CrAT (V459T and N514R), and the resulting ChAT mutant showed an increase in catalytic efficiency toward carnitine. In addition to electrostatic factors, the crystal data also indicate that steric factors might contribute to the selectivity of ChAT toward choline rather than carnitine.

In the present study, we have identified a new amino acid ($Asp^{356}$ in rat CrAT) that could contribute, along with $Met^{564}$, to acyl-CoA selectivity in CrAT. Enzyme activity and kinetic parameters of the yeast-expressed rat CrAT double mutant D356A/M564G show that it has a preference for palmitoyl-CoA as the substrate rather than its natural substrate acetyl-CoA. Furthermore, to redesign rat CrAT specificity from carnitine to choline, we replaced four amino acids in rat CrAT with their counterparts in ChAT (A106M, T465V, T467N, and R518N) by site-directed mutagenesis. The modified CrAT shows an increase in catalytic efficiency toward choline and a decrease in catalytic efficiency toward carnitine compared with that of the wt enzyme.

## EXPERIMENTAL PROCEDURES

*Construction of Rat CrAT and CPT I Models.* A structural model of wt CrAT enzyme was constructed by homology modeling techniques using as templates the structures deposited in the Protein Data Bank (pdb) corresponding to human (1NM8) (*13*) and mouse CrAT (1NDB, 1NDF, and 1NDI) (*12*), essentially as described elsewhere (*15*). The model of liver CPT I (L-CPT I) was constructed using as a template the structure of mouse carnitine octanoyltransferase (1XL7, 1XL8) (*14*), essentially as described elsewhere (*22*). CrAT mutants M564G, D356A/M564G, T465V/T467N/R518N, and A106M/T465V/T467N/R518N were modeled by the same procedures using the rat wt CrAT model as the template. The structural quality of the models was checked using the WHAT-CHECK routines (*23*) from the WHAT IF program (*24*) and the PROCHECK validation program from the SWISS-MODEL server facilities (*25*). The 3-D coordinates of the rat ChAT structure were obtained from the pdb entries 1Q6X (*17*) and 1T1U (*18*).

*Molecular Docking.* Structural models of the molecular interaction between the substrates myristoyl-CoA ($C_{14}$-CoA), palmitoyl-CoA ($C_{16}$-CoA), stearoyl-CoA ($C_{18}$-CoA), and arachidoyl-CoA ($C_{20}$-CoA) and the 3-D models of the putative receptor mutant proteins of rat CrAT M564G and D356A/M564G were built using the suite of programs included in the Autodock package (*26*, *27*). The proteins and acyl-CoA ligands were prepared using standard procedures as specified in the package documentation. To ensure a complete search of binding sites available for acyl-CoAs, independent docking calculations were performed. To intensively sample their conformational space, we used the whole set of rotatable bonds in the acyl chains of the ligands. Only docking models with their CoA residue positions close to those found in the 1NDI crystal (*12*) were considered for further steps. Finally, among the position clusters selected for each ligand, the model with the lowest docking energy for each particular interaction was considered. The putative palmitoyl-CoA binding site in rat wt L-CPT I was modeled on the basis of information from the docking procedures using the AutoDock docking program, essentially as described elsewhere (*22*). The structural interactions between the substrates choline and carnitine and the rat wt ChAT, wt CrAT, and CrAT mutant proteins T465V/T467N/R518N (triple mutant, TM) and A106M/T465V/T467N/R518N (quadruple mutant, QM), respectively, were performed using the methods implemented in the Autodock suite. To preserve the structural position and conformation of carnitine and choline, respectively, within the active sites indicated in the original publications of CrAT and ChAT structures (*12, 17, 18*), rigid docking models were obtained for every putative

interaction. Only docked models locating the common trimethylammonium group of both choline and carnitine in the sites originally suggested were considered for refining. As in the case of the acyl-CoA substrates, the lowest energy docked models were selected within the filtered sets.

*Construction of Site-Directed Mutants of Rat CrAT.* Plasmids pYESCrAT$^{M564G}$ and pGEX-CrAT$^{wt}$ were obtained as previously described (*15*). CrAT mutant D356A/M564G was constructed using the Quick Change PCR-based mutagenesis procedure (Stratagene) with the pYESCrAT$^{M564G}$ plasmid as the template. CrAT mutant T465V/T467N was obtained using the pGEX-CrAT$^{wt}$ plasmid as the template; CrAT mutant T465V/T467N/R518N was constructed using the pGEX-CrAT$^{T465V/T467N}$ plasmid as the template and CrAT mutant A106M/T465V/T467N/R518N was constructed using the pGEX-CrAT$^{T465V/T467N/R518N}$ plasmid as the template. The appropriate substitutions as well as the absence of unwanted mutations were confirmed by sequencing the inserts.

*Expression of Rat CrAT and L-CPT I in Saccharomyces cerevisiae.* Plasmids containing wt L-CPT I and CrAT mutants M564G and D356A/M564G were expressed in yeast cells, and mitochondrial cell extracts were prepared as previously described (*28*). A *S. cerevisiae* strain devoid of COT and CPT activity and lacking the endogenous CAT2 gene (FY23Δ*cat2* (MATa trp1 ura3 Δ*cat2*::LEU2)) was used as an expression system (*29*).

*Expression and Purification of Rat CrAT in Escherichia coli.* For expression and purification of rat CrAT wt and CrAT triple mutant T465V/T467N/R518N and quadruple mutant A106M/T465V/T467N/R518N, the glutathione S-transferase (GST) gene fusion system (Amersham Biosciences) was used. The pGEX-6P-1 plasmids containing wt CrAT and mutant CrAT were transformed into *E. coli* BL21, and fusion protein GST-CrAT was overexpressed overnight after the addition of 0.1 mM of isopropyl-1-thio-β-D-galactopyranoside (IPTG) at 18 °C. The soluble fusion protein was purified from bacterial lysates using glutathione-sepharose 4B with a batch method. Finally, CrAT was eluted by cleavage of the fusion protein with the site-specific protease PreScission protease. The eluted protein contains five additional amino acids (Gly-Pro-Leu-Gly-Ser) at its *N*-terminus before the ATG start codon.

*Determination of Enzymatic Activity.* Two methods were used for the assay of carnitine acyltransferase: an endpoint fluorometric method (*30*) and a radiometric method (*28*). The fluorometric assay was used in all cases, unless otherwise indicated.

*Fluorometric Method.* The forward reaction of carnitine acyltransferase activity was assayed for 8 min at 30 °C in a solution containing 0.1 mM acyl-CoA, 1.5 mM EDTA, 1.5 mM L-carnitine, and 40 mM Hepes buffer at pH 7.8, in a total volume of 600 μL. The reactions were started by the addition of 5 μg of yeast-expressed CrAT or from 0.1 to 1 μg of *E. coli*-expressed CrAT. Parallel (blank) assays were run in the absence of L-carnitine or choline. All fluorometer recordings were performed with a Perkin-Elmer LS 45 luminescence spectrometer, and the enzyme activities were measured in duplicate. For the determination of the $K_m$ value for carnitine or choline, acyl-CoA was fixed at 0.1 mM. For the determination of the $K_m$ value for acyl-CoA, the choline concentration was fixed at 100 mM, and the carnitine concentration was fixed at 1.5 mM (wt and CrAT mutant D356A/M564G) or 100 mM (CrAT triple mutant T465V/T467N/R518N and quadruple mutant A106M/T465V/T467N/R518N). Carnitine was neutralized with KOH before use. The values reported are the means and standard deviations of three determinations. Protein concentrations were measured using the Bio-Rad protein assay with BSA as standard. The $K_m$ and $V_{max}$ values were determined by fitting the data using nonlinear regression analysis to the Michaelis−Menten equation with Sigma Plot software. Catalytic efficiency was defined as $V_{max}/K_m$ for yeast-expressed CrAT and as the $K_{cat}/K_m$ for *E.coli*-expressed CrAT.

*Radiometric Method.* This assay was used to compare CrAT double mutant D356A/M564G and L-CPT I wild-type activities in mitochondria-enriched fractions (5 μg) obtained from yeast. The forward reaction of carnitine acyltransferase activity was assayed for 4 min at 30 °C in a total volume of 200 μL as previously described (28). The substrates were 400 μM L-[*methyl*-$^3$H]carnitine and 50 μM acyl-CoAs of varying length, ranging from hexanoyl-CoA ($C_6$-CoA) to arachidoyl-CoA ($C_{20}$-CoA).

*Immunological Techniques.* The mitochondrial protein (8 μg) from *S. cerevisiae* expressing CrAT was treated with the sample buffer and subjected to 8% (w/v) SDS−PAGE. Electroblotting to nitrocellulose sheets was carried out for 1 h at 250 mA. The immunodetection of CrAT was performed using anti-rat CrAT antibodies (1:10 000 dilution) (*15*). The blots were developed with the ECF Western blotting system (Amersham Biosciences). The quantifications were carried out using a fluorescence scanning device from Molecular Dynamics Storm 840.

## RESULTS AND DISCUSSION

*Re-Engineering CrAT into a Pseudo CPT.* In an earlier study, we showed that the amino acid Met$^{564}$ of rat CrAT was critical to fatty acyl-chain-length specificity in CrAT (*15*) because its mutation to glycine (CrAT mutant M564G) broadened CrAT acyl-CoA specificity from short-chain acyl-CoAs to medium-chain acyl-CoAs; indeed, we transformed rat CrAT into a pseudo COT. We also constructed a 3-D model of the location of fatty acyl-CoAs in the active center of wt and mutated M564G CrAT. After a thorough examination of the 3-D model for the positioning of myristoyl-CoA in the CrAT M564G mutant, we identified one charged residue, Asp$^{356}$, which conforms the putative bottom closure of the hydrophobic pocket that could sterically hinder the correct positioning of longer acyl-CoAs than myristoyl-CoA, such as palmitoyl-CoA. To create a more suitable environment for the acyl group of long-chain acyl-CoAs inside the hydrophobic pocket of CrAT, we mutated Asp$^{356}$ to the small, uncharged hydrophobic residue Ala. We prepared the double CrAT mutant D356A/M564G, which was expressed in a *S. cerevisiae* strain devoid of endogenous CrAT, COT, and CPT activity. Enzyme activity of the yeast-expressed CrAT mutant D356A/M564G was tested for acyl-CoA substrates of various lengths from acetyl-CoA to arachidoyl-CoA and compared with that of the CrAT mutant M564G. As previously described (*15*), CrAT mutant M564G (Table 1) was very active toward medium-chain acyl-CoAs, especially hexanoyl-CoA, but much less active toward palmitoyl-CoA (802 and 18.0 nmol·min$^{-1}$·mg protein$^{-1}$, respectively), and its activity with longer acyl-CoAs (stearoyl- and arachidoyl-CoA) was

Table 1: Enzyme Activities of Rat CrAT wt and Mutants M564G and D356A/M564G Expressed in *Saccharomyces cerevisiae*[a]

| | activity (nmol·min$^{-1}$·mg protein$^{-1}$) | | |
|---|---|---|---|
| acyl-CoA | CrAT wt | CrAT M564G | CrAT D356A/M564G |
| $C_2$-CoA | 409 ± 48 | 234 ± 30 | 50.7 ± 4.0 |
| $C_4$-CoA | 518 ± 19 | 641 ± 3.2 | 138 ± 26 |
| $C_6$-CoA | 138 ± 15 | 802 ± 66 | 246 ± 15 |
| $C_8$-CoA | 61 ± 1.1 | 488 ± 24 | 127 ± 29 |
| $C_{10}$-CoA | 20.7 ± 5.7 | 136 ± 7.3 | 67.0 ± 0.7 |
| $C_{12}$-CoA | 6.0 ± 2.6 | 350 ± 5.0 | 150 ± 24 |
| $C_{14}$-CoA | 0.33 ± 0.07 | 409 ± 29 | 218 ± 9.0 |
| $C_{16}$-CoA | UD | 18.0 ± 3.6 | 100 ± 19 |
| $C_{18}$-CoA | UD | UD | 38.9 ± 1.4 |
| $C_{20}$-CoA | UD | UD | UD |

[a] The mitochondrial protein from yeast expressing wt CrAT and CrAT mutants M564G and D356A/M564G were assayed with acyl-CoAs of different carbon length ranging from $C_2$−$C_{20}$ as described in Experimental Procedures. The results are the mean ± SD of at least three independent experiments with different preparations. UD represents the undetectable activity.

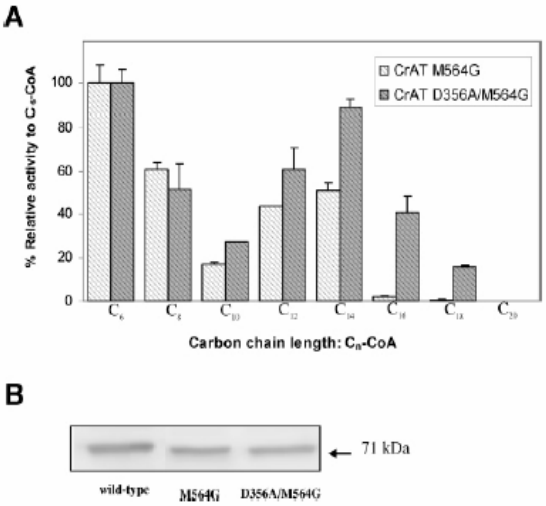


FIGURE 1: Carnitine acetyltransferase activity of *S. cerevisiae* cells expressing CrAT mutant M564G and double mutant D356A/M564G. (A) Extracts from yeast expressing CrAT mutant M564G and double mutant D356A/M564G were assayed for activity with acyl-CoAs of different chain length ranging from $C_6$−$C_{20}$, as described in Experimental Procedures. The results are expressed as the relative acyl-CoA activity with regard to hexanoyl-CoA activity (scaled to 100). The results are the mean ± SD of at least three independent experiments with different preparations. (B) Immunoblots showing expression of wt CrAT, CrAT M564G, and CrAT D356A/M564G. *S. cerevisiae* extracts (8 $\mu$g) were separated by SDS−PAGE and subjected to immunoblotting using specific antibodies. The arrows indicate the migration position and the molecular mass of rat CrAT (71 kDa).

undetectable. CrAT double mutant D356A/M564G also showed maximum activity toward hexanoyl-CoA (246 nmol·min$^{-1}$·mg protein$^{-1}$), but in contrast, it showed a 6-fold increase in activity toward palmitoyl-CoA (100 nmol·min$^{-1}$·mg protein$^{-1}$) and a new activity toward stearoyl-CoA (38.9 nmol·min$^{-1}$·mg protein$^{-1}$) compared with that of the single mutant M564G. If we express the results for palmitoyl-CoA as its relative activity with respect to hexanoyl-CoA, this figure was 41% for the CrAT double mutant but only 2% for the single mutant (Figure 1A).

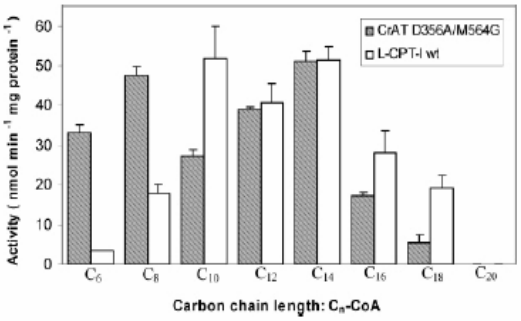


FIGURE 2: Carnitine acyltransferase activity of *S. cerevisiae* cells expressing L-CPT I wild type and CrAT double mutant D356A/M564G. The mitochondrial protein from yeast expressing L-CPT I and CrAT double mutant D356A/M564G were assayed for activity using a radiometric method with acyl-CoAs of different chain length ranging from $C_6$−$C_{20}$, as described in Experimental procedures. The results are the mean ± SD of at least three independent experiments with different preparations.

Table 2: Kinetic Parameters of Rat CrAT Mutant D356A/M564G Expressed in *Saccharomyces cerevisiae*[a]

| acyl-CoA | $K_m$ ($\mu$M) | $V_{max}$ (nmol·min$^{-1}$·mg protein$^{-1}$) | catalytic efficiency ($V_{max}/K_m$) |
|---|---|---|---|
| $C_2$-CoA | 23.0 ± 3.1 | 66.5 ± 2.1 | 2.9 |
| $C_{16}$-CoA | 7.2 ± 0.4 | 138 ± 25 | 19.2 |

[a] Mitochondrial protein from yeast expressing CrAT mutant D356A/M564G was assayed with acetyl- and palmitoyl-CoA, as described in Experimental Procedures. The results are the mean ± SD of at least three independent experiments with different preparations.

In addition, yeast-expressed CrAT double mutant D356A/M564G and L-CPT I wt activities were compared using a radiometric method with acyl-CoAs of different length from $C_6$-CoA to $C_{20}$-CoA (Figure 2). The CrAT double mutant showed exactly the same activity as that of L-CPT I when $C_{12}$-CoA and $C_{14}$-CoA were used as substrates. In longer acyl-CoAs, the CrAT double mutant displayed a similar activity toward palmitoyl-CoA, approximately 65% of that of L-CPT I wt (17.8 vs 28 nmol·min$^{-1}$·mg protein$^{-1}$, respectively), whereas its activity with stearoyl-CoA was 25% of that of L-CPT I wt. The CrAT double mutant still maintained strong activity with $C_6$ and $C_8$-CoA as substrates, whereas the L-CPT I activity toward acyl-CoAs with fewer than 10 carbons in their chain was much lower.

These results indicate that the replacement of Asp$^{356}$, which conforms the bottom closure of the acyl-CoA binding pocket of CrAT by alanine (D356A) along with the mutation of Met$^{564}$ to Gly, allows CrAT to catalyze long-chain acyl-CoAs such as palmitoyl- and stearoyl-CoA. CrAT double mutant D356A/M564G catalyzes acyl-CoAs of a wide range of chain length, from acetyl-CoA to stearoyl-CoA.

Moreover, we determined the kinetic parameters of the CrAT mutant D356A/M564G with its novel substrate palmitoyl-CoA and its natural substrate acetyl-CoA (Table 2). The mutant showed standard saturation kinetics for both acyl-CoAs. The $K_m$ values with acetyl-CoA and palmitoyl-CoA were 23 and 7.2 $\mu$M, respectively, indicating a preference for long-chain acyl-CoAs. Furthermore, the $K_m$ value of this double mutant with palmitoyl-CoA was very similar to that of L-CPT I wt, 5.7 $\mu$M (*22*). When acetyl-CoA was the substrate, the catalytic efficiency (defined as $V_{max}/K_m$ ratio)

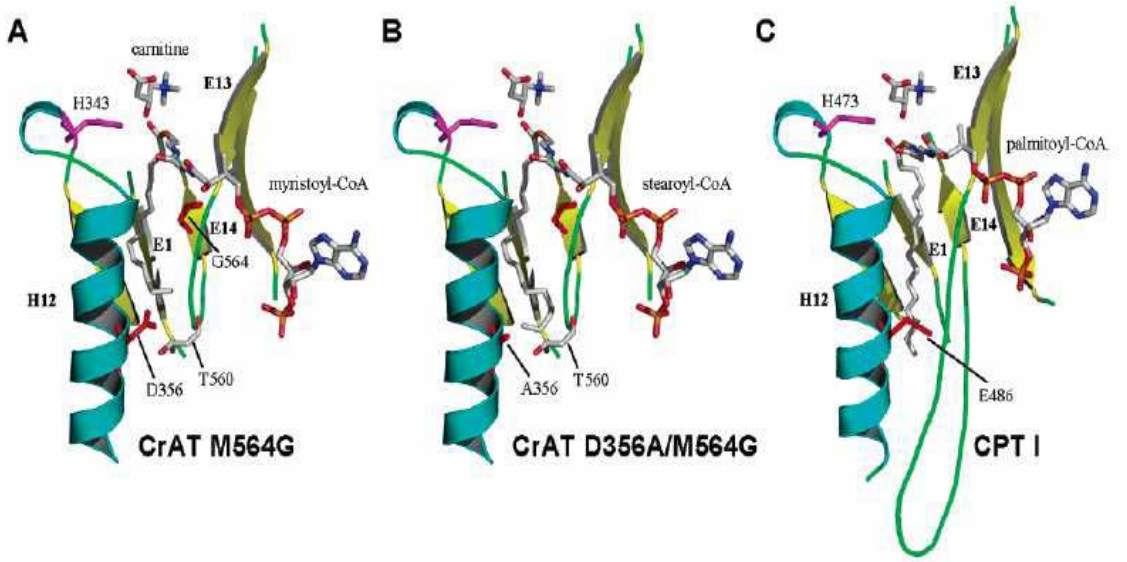


FIGURE 3: Proposed models for the positioning of long-chain acyl-CoAs in CrAT mutants M564G and D356A/M564G and wt L-CPT I. (A) Location of a myristoyl-CoA molecule in the pocket opened in CrAT mutant M564G. (B) Location of a stearoyl-CoA molecule (showing a U-turn of the ending carbon atom bonds) in the deep pocket open in CrAT mutant D356A/M564G. The position of residues $Gly^{564}$ and $Asp^{356}$ or $Ala^{356}$ (red) as well as $Thr^{560}$, the catalytic $His^{343}$ (magenta), and the molecule of carnitine are indicated. Secondary structure elements of the active center surrounding the acyl chain locus are also represented (alpha helix H12 in blue, beta strands in yellow). (C) Model for the location of a molecule of palmitoyl-CoA in CPT I. The presence of charged $Glu^{486}$ does not interfere with the substrate position because of the wider cavity conformed by the naturally adopted structural elements, including the distinctive long and flexible loop between beta strands E13 and E14.

was 2.9, whereas with palmitoyl-CoA, it was 19.2, which again shows that the double CrAT mutant prefers long-chain acyl-CoAs. Western blot of yeast-expressed wt CrAT and mutants D356A/M564G and M564G showed the same molecular masses and similar expression levels (Figure 1B).

*Positioning of Long-Chain Acyl-CoAs in CrAT Mutant D356A/M564G.* In a previous study (15), a 3-D model was proposed for the location of myristoyl-CoA in the hydrophobic pocket of the CrAT single mutant M564G. Refined in silico docking techniques were used in the present study, allowing the free rotation of the acyl chain bonds of the ligands. This ensured a complete scan of the available conformational space inside the enzyme cavity. The new model for the position of myristoyl-CoA is similar to the published model (*15*), locating the acyl chain in the cavity that is open when $Met^{564}$ is replaced by glycine. The bottom of the pocket is defined by the presence of $Thr^{560}$, which closes the enzyme wall to the external surface and $Asp^{356}$, which prevents the correct positioning of acyl-CoAs longer than myristoyl-CoA (Figure 3A).

The bigger cavity formed in CrAT mutant D356A/M564G by replacing the larger, charged $Asp^{356}$ by the tiny, nonpolar alanine, allows the positioning of longer-chain acyl-CoAs. This has also been calculated, using the same in silico docking method, for palmitoyl-CoA ($C_{16}$-CoA) (data not shown) and stearoyl-CoA ($C_{18}$-CoA) (Figure 3B). The last four carbon atoms of the acyl chain of stearoyl-CoA form a U-turn, which avoids collision with $Thr^{560}$ at the bottom of the tunnel and accommodates them in the space available around the substituted $Ala^{356}$.

When the docking of very long-chain acyl-CoAs, such as arachidoyl-CoA ($C_{20}$-CoA), into the large cavity of the CrAT D356A/M564G mutant was carried out, no models with low (stable) energy were obtained despite using the minimum constraints of the appropriate location of the substrate to the enzyme active center. This indicates that the available space was too small to accommodate acyl chains of more than 18 atoms in length. The U-turn formed by stearoyl-CoA points toward the residues in the alpha helix H12 (Figure 3B), leaving no free space for additional carbon atoms of longer acyl chains. The absence of an appropriate model is consistent with the lack of activity of the D356A/M564G mutant enzyme toward arachidoyl-CoA (Figure 1A).

Taking into account all of the previous results, we propose a model for the acyl-CoA chain-length discrimination in CrAT on the basis of the presence of two amino acids, $Met^{564}$ and $Asp^{356}$, which act as checkpoints at different stages of the entry of acyl-CoAs to the fatty acid binding site. The bulkier side chain of $Met^{564}$ forms the floor of the shallow fatty acid binding pocket of CrAT and impedes the entry of medium- and long-chain acyl-CoAs, which explains CrAT selectivity for short-chain acyl-CoAs. The replacement of this Met by the smaller Gly (M564G) opens the binding site and reveals a deeper hydrophobic pocket that can accommodate acyl-CoAs of up to 14 carbons. The hydrophobic chain of longer acyl-CoAs cannot fit in the pocket, in the presence of the side chain of charged $Asp^{356}$ and, therefore, cannot be catalyzed by the enzyme. The substitution of this amino acid by a smaller, noncharged residue (D356A) along with the M564G mutation, completely opens the binding site and allows the entry of long-chain acyl-CoAs, such as palmitoyl- and stearoyl-CoA.

It has to be noted that the replacement of $Met^{564}$ by Gly is based on both structural and sequence alignment considerations (Met is replaced by Gly in COTs and CPTs), and this substitution could be considered as an evolutionary

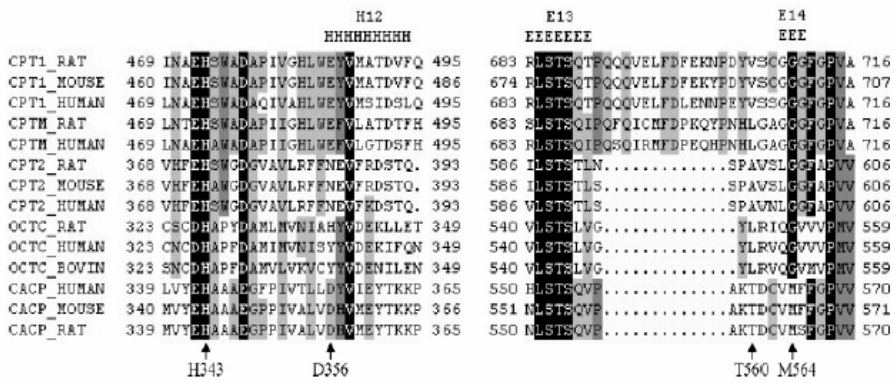


FIGURE 4: Alignment of representative sequences of structure elements surrounding the acyl chain locus of carnitine acyltransferases. The amino acid sequence of 14 representative enzymes that catalyze short acyl-CoAs as substrates: CrAT (CACP) from humans, mice, and rats; and enzymes which have medium- and long-chain acyl-CoAs as substrates: L-CPT I (CPT1) from rats, mice, and humans; M-CPT I (CPTM) from humans and rats; CPT II (CPT2) from rats, mice, and humans; and COT (OCTC) from humans, rats, and bovines were obtained from the SwissProt data bank and aligned using ClustalW. The residues are colored according to conservation. The CrAT $Asp^{356}$ residue corresponds to His or Tyr for COT ($His^{340}$ or $Tyr^{340}$), and for CPT I, it is a glutamic ($Glu^{486}$), and for CPT II, it is an asparagine ($Asn^{385}$). The position of catalytic histidine (CrAT $His^{343}$) and the conserved residue according to acyl-chain-length specificity (for CrAT, it is a methionine -$Met^{564}$-, and for COT and CPTs, it is a glycine) are also noted. The secondary structure elements alpha helix H12 and beta strands E13 and E14 are indicated.

development that was selected because it enabled the carnitine acyltransferase family to catalyze longer acyl-CoAs. However, our replacement of the $Asp^{356}$ by Ala was only based on structural considerations. Alignment of the proteins of the family shows high variability in the zone close to the $Asp^{356}$, and the orthologous residues corresponding to CrAT $Asp^{356}$ are His/Tyr in COT, Asn in CPT II, and Glu in CPT I (Figure 4). In these enzymes, naturally conformed to accept long chain substrates, the cavity has adopted a shape slightly different to that of acetyltransferases. Small displacements of beta strands E1 and E13 as well as alpha helix H12 lead to a wider cavity where long substrates can adopt less restrictive conformations. This situation may be extrapolated from CPT I models (*22*), and it was observed in mouse COT structures (*14*). Therefore, the presence of bulky or charged residues in this position for long-chain enzymes is not so critical in terms of substrate fitting as it is for mutated carnitine acetyltransferases, which carry a narrower, hidden cavity. The mutation of $Asp^{356}$ to Ala along with the mutation of $Met^{564}$ to Gly creates an artificial enzyme that behaves as a CPT in terms of acyl-CoA specificity, although it is clear that the replacement of this $Asp^{356}$ by Ala is not the strategy followed by nature to handle long-chain substrates in CPTs, in contrast to the replacement of $Met^{564}$ by Gly. The selectivity for long-chain substrates may be determined by more complicated factors than specific amino acid variations between the different members of the family, possibly by the interactions among several different residues, and, at the same time, by variations in secondary structural elements. The most striking difference in the CPT I enzymes is the presence of a 13-amino acid insertion between beta strands E13 and E14 (Figure 4) that may form a more flexible pocket that can accommodate long-chain acyl groups (Figure 3C). Interestingly, this insertion is located just before the $Met^{564}$ residue.

As suggested by in silico modeling procedures, the cavity opened in the D356A/M564G mutant is almost completely occupied when stearoyl-CoA is introduced. Even allowing the full rotation of acyl chain bonds, it was impossible to obtain an active-enzyme compatible model for longer substrates. The longer substrates could perhaps be accommodated in the hydrophobic pocket if the side chain of $Thr^{560}$ were to be removed. However, the fact that this residue is part of the external surface of the protein introduces new variables (e.g., contacts of the end of the acyl chain with surrounding water), which makes it difficult to develop a model using current in silico methodologies.

*Choline−Carnitine Discrimination in Rat CrAT.* Taking into consideration all of the structural information revealed by the recent publication of the rat ChAT crystal (*17*, *18*) and the mutagenesis studies performed by Cronin (*19*), we attempted to redesign CrAT to use choline as the acceptor of the acetyl group instead of its natural substrate carnitine. First, we prepared the CrAT triple mutant T465V/T467N/R518N (TM), which incorporates the reverse substitutions that Cronin successfully performed in rat ChAT and allowed him to accommodate carnitine instead of choline. The triple mutant was expected to eliminate most of the interactions between the enzyme and the carboxylate group of carnitine, which might favor the binding of choline. At the same time, however, this triple mutant might increase the volume of the catalytic site of CrAT, which could interfere with the correct positioning of the smaller choline. Therefore, to reduce the volume of the carnitine binding pocket and create a more favorable environment to accommodate the choline, we prepared the CrAT quadruple mutant A106M/T465V/T467N/R518N (QM) with the additional replacement of $Ala^{106}$ with Met. CrAT TM and QM were expressed in *E. coli*, and the protein was purified to homogeneity. Kinetic experiments were performed with the substrate pairs choline/acetyl-CoA and carnitine/acetyl-CoA (Table 3). The wt enzyme and both mutants showed standard saturation kinetics for all of the substrates tested, with the exception of the quadruple mutant with carnitine.

Both CrAT mutants showed improved catalytic efficiency toward choline ($K_{cat}/K_m$) compared with that of the wt, and this increase was higher in the QM (9-fold) than in the TM (5-fold). In both mutants, the increase in catalytic efficiency was more influenced by the lowering of the $K_m$ value toward

Table 3: Kinetic Parameters of Rat CrAT in *Escherichia coli* Cells Expressing CrAT Wild-Type, Triple Mutant T465V/T467N/R518N and Quadruple Mutant A106M/T465V/T467N/R518N[a]

| | $K_m$ ($\mu$M) | | $K_{cat}$ ($s^{-1}$) | | catalytic efficiency ($K_{cat}/K_m$) ($M^{-1}s^{-1}$) | |
|---|---|---|---|---|---|---|
| CrAT | carnitine | choline | carnitine | choline | carnitine | choline |
| wt | 101 ± 4.6 | 86400 ± 5300 | 86.9 ± 3.6 | 1.58 ± 0.14 | $8.6 \times 10^5$ | 18.2 |
| TM | 260000 ± 19000 | 29000 ± 4200 | 2.97 ± 0.07 | 2.43 ± 0.10 | 11.4 (↓ 75000) | 83.7 (↑ 5) |
| QM | >300000 | 18100 ± 330 | 0.98 ± 0.08 | 3.11 ± 0.19 | 1.34 (↓ 640000) | 172 (↑ 9) |

[a] Purified protein from *E. coli* expressing CrAT wild-type (wt) and mutants T465V/T467N/R518N (TM) and A106M/T465V/T467N/R518N (QM) were assayed for kinetics as described in Experimental Procedures. The results are the mean ± SD of three independent experiments with different preparations. The values in parentheses represent the fold change of catalytic efficiency ($K_{cat}/K_m$) versus that of the wild-type.

choline (5-fold in the QM and 3-fold in the TM) than by an increase in the $K_{cat}$ value.

In contrast with the results obtained with choline, the two mutants reduced the catalytic efficiency toward carnitine. Again, the greatest effect occurred with the quadruple mutant, with a decrease of more than 5 orders of magnitude (640 000-fold) in catalytic efficiency in comparison with that of wt, whereas the reduction in the triple mutant was about 75 000-fold. This impairment in catalytic efficiency toward carnitine is due to the combination of a decrease in the $K_{cat}$ value and an increase in the $K_m$ value toward carnitine, the latter being the stronger factor.

The comparison of the catalytic efficiencies between choline and carnitine for each enzyme derivative shows that although CrAT wt prefers carnitine over choline as the acceptor of the acetyl moiety by a factor of 47 000 ($8.6 \times 10^5$ vs. 18.2 $M^{-1}s^{-1}$) the mutation of four amino acid residues in CrAT shifts the catalytic discrimination of the enzyme in favor of choline. Thus, the QM acetylates choline with a higher catalytic efficiency than carnitine by a factor of 128 (172 vs 1.34 $M^{-1}s^{-1}$).

In the CrAT triple and quadruple mutants, the $K_m$ values for acetyl-CoA in the presence of carnitine and choline were very similar to those of wt CrAT. When carnitine was used, the $K_m$ values for acetyl-CoA were 39 $\mu$M for wt CrAT, 33 $\mu$M for the TM, and 28 $\mu$M for the QM. In the presence of choline, the $K_m$ values for acetyl-CoA were 19 $\mu$M for wt CrAT, 26 $\mu$M for the TM, and 28 $\mu$M for the QM. These results indicate that none of the mutations had any effect on the affinity of the enzyme for acetyl-CoA.

Our results indicate two factors that contribute to the discrimination between choline and carnitine in CrAT to a similar extent. The first factor is the electrostatic interaction of $Thr^{465}$ and $Arg^{518}$ with the carboxylate group of carnitine. When this interaction is eliminated in the CrAT triple mutant, its catalytic efficiency toward carnitine dramatically decreases, and there is a 5-fold increase in catalytic efficiency toward choline. The second factor is the side-chain volume of the residues around the carnitine in the active site of CrAT. The replacement of $Ala^{106}$ in CrAT by methionine in the quadruple mutant reduces the volume of the carnitine binding site, which almost completely blocks carnitine acetyltransferase activity and increases the catalytic efficiency toward choline by 9-fold, nearly doubling the effect of the abolition of the electrostatic interactions.

In an attempt to understand the characteristics of the carnitine/choline binding site in CrAT, 3-D models were built for the wt and the triple and quadruple CrAT mutants and compared with the published structures of rat ChAT (*17*, *18*). Using rigid docking techniques, the location of both substrates was calculated for each enzyme active center (Figure 5). According to the models, the electrostatic characteristics of the substrate site for TM CrAT resemble wt ChAT more than wt CrAT. In addition to the lack of specific contact for the carboxylate group of carnitine, the site for the trimethylammonium group, common for both substrates, is maintained. In the quadruple mutant, the presence of Met instead of the original $Ala^{106}$ almost completely mimics the wt ChAT active site. We conclude that the reduction of the size of the tunnel impedes the entry of carnitine and allows better positioning of the smaller choline.

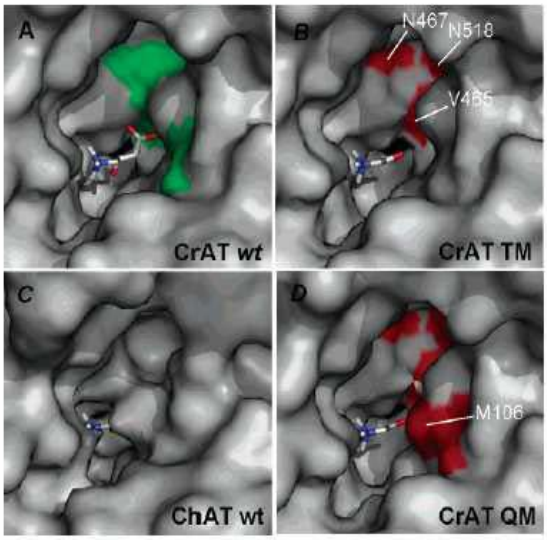


FIGURE 5: Models of substrate binding sites for wt CrAT, CrAT TM, and CrAT QM compared to the active site of rat wt ChAT. The representation of the protein surface of the entrance tunnel for carnitine/choline substrates for (A) rat CrAT wt, (B) CrAT triple mutant (T465V/T467N/R518N), (C) wt ChAT structure, and (D) CrAT quadruple mutant (A106M/T465V/T467N/R518N). The location of a molecule of carnitine is represented in the wt CrAT model, whereas a molecule of choline is represented in CrAT TM, CrAT QM, and wt ChAT. The vacuum electrostatics for active sites was calculated and represented using PyMOL (*33*). The approximate positions of mutated residues $Met^{106}$, $Val^{465}$, $Asn^{467}$, and $Asn^{518}$ are indicated in red. Green shows the approximate positions of $Ala^{106}$, $Thr^{465}$, $Thr^{467}$, and $Arg^{518}$ in wt CrAT.

The fact that our improvement of the catalytic efficiency of CrAT toward choline (9-fold) was not as successful as that achieved by Cronin (*19*) with ChAT toward carnitine (1620-fold) is not due to a failure in the acquisition of choline activity of CrAT mutants because their catalytic activity with

choline is only 3 times lower than that of mutant ChAT with carnitine (172 vs 469 $M^{-1}s^{-1}$). The discrepancy is attributable to the fact that wt CrAT is very active toward choline ($K_{cat}/K_m$ = 18.2 $M^{-1}s^{-1}$), whereas wt ChAT has a very low carnitine acetyltransferase activity ($K_{cat}/K_m$ = 0.289 $M^{-1}s^{-1}$). The relatively high choline acetyltransferase activity of wt CrAT could be due to the fact that choline can enter the carnitine binding pocket without any steric hindrance. The amino acid substitutions in rat CrAT in this study disclose several residues that are involved in acyl-CoA and choline substrate recognition and provide insight into the molecular requirements for their correct positioning for an efficient catalysis.

The carnitine acyltransferase family has received much attention because they are considered promising targets for the development of drugs against type II diabetes and other human diseases (*31*, *32*). CrAT mutant D356A/M5464G catalyzes acyl-CoAs over a wide range of chain length, from acetyl- to palmitoyl-CoA, thereby mimicking the natural proteins CrAT, COT, and CPT. Long-chain acyl-CoAs (LC-CoAs) are candidate mediators of insulin resistance. Therefore, this double mutant may be useful for studies of the influence of fatty acids on insulin resistance. If this CrAT double mutant were to be overexpressed, these harmful LC-CoAs would be transformed into acylcarnitine derivatives and then excreted in urine, thus detoxifying selective acyl residues and releasing free CoA and modulating the CoA/acyl-CoA ratio. The overexpression of this mutant CrAT presents two advantages over the overexpression of CPT I. First, CrAT mutant D356A/M564G reacts with a broader series of fatty acid acyl-CoAs than CPT I and facilitates the excretion of a wider range of harmful acyl residues as acylcarnitines. Second, CrAT mutant D356A/M5464G activity is not inhibited by malonyl-CoA (data not shown): at variance with wt CPT I but the same as wt CrAT. The results presented in this study not only help us to understand the structure/function relationship within the acyltransferase family, but also facilitate studies on obesity, noninsulin-dependent diabetes (NIDDM), and defective $\beta$-oxidation.

## ACKNOWLEDGMENT

We are grateful to Robin Rycroft of the Language Service for valuable assistance in the preparation of the English manuscript.

## REFERENCES

1. Miyazawa, S., Ozasa, H., Furuta, S., Osumi, T., and Hashimoto, T. (1983) Purification and properties of carnitine acetyltransferase from rat liver, *J. Biochem. (Tokyo) 93*, 439−451.
2. Miyazawa, S. Ozasa, H., Osumi, T., and Hashimoto, T. (1983) Purification and properties of carnitine octanoyltransferase and carnitine palmitoyltransferase from rat liver, *J. Biochem. (Tokyo) 94*, 529−542.
3. McGarry, J. D., and Brown, N. F. (1997) The mitochondrial carnitine palmitoyltransferase system. From concept to molecular analysis, *Eur. J. Biochem. 244*, 1−14.
4. Bieber, L. L., Krahling, J. B., Clarke, P. R., Valkner, K. J., and Tolbert, N. E. (1981) Carnitine acyltransferases in rat liver peroxisomes, *Arch. Biochem. Biophys. 211*, 599−604.
5. Zammit, V. A. (1999) Carnitine acyltransferases: functional significance of subcellular distribution and membrane topology, *Prog. Lipid. Res. 38*, 199−224.
6. Bieber, L. L. (1988) Carnitine, *Annu. Rev. Biochem. 57*, 261−283.
7. Kalaria, R. N., and Harik, S. I. (1992) Carnitine acetyltransferase activity in the human brain and its microvessels is decreased in Alzheimer's disease, *Ann. Neurol. 32*, 583−586.
8. DiDonato, S., Rimoldi, M., Moise, A., Bertagnoglio, B., and Uziel, G. (1979) Fatal ataxic encephalopathy and carnitine acetyltransferase deficiency: a functional defect of pyruvate oxidation? *Neurology 29*, 1578−1583.
9. Brevetti, G., Angelini, C., Rosa, M., Carrozzo, R., Perna, S., Corsi, M., Matarazzo, A., and Marcialis, A. (1991) Muscle carnitine deficiency in patients with severe peripheral vascular disease, *Circulation 84*, 1490−1495.
10. Melegh, B., Seress, L., Bedekovics, T., Kispal, G., Sümegi, B., Trombitas, K., and Mehes, K. (1999) Muscle carnitine acetyltransferase and carnitine deficiency in a case of mitochondrial encephalomyopathy, *J. Inherited Metab. Dis. 22*, 827−838.
11. An, J., Muoio, D. M., Shiota, M., Fujimoto, Y., Cline, G. W., Shulman, G. I., Koves, T. R., Stevens, R., Millington, D., and Newgard, C. B. (2004) Hepatic expression of malonyl-CoA decarboxylase reverses muscle, liver and whole-animal insulin resistance, *Nat. Med. 10*, 268−274.
12. Jogl, G., and Tong, L. (2003) Crystal structure of carnitine acetyltransferase and implications for the catalytic mechanism and fatty acid transport, *Cell 112*, 113−122.
13. Wu, D., Govindasamy, L., Lian, W., Gu, Y., Kukar, T., Agbandje-McKenna, M., and McKenna, R. (2003) Structure of human carnitine acetyltransferase. Molecular basis for fatty acyl transfer, *J. Biol. Chem. 278*, 13159−13165.
14. Jogl, G., Hsiao, Y., and Tong, L. (2005) Crystal structure of mouse carnitine octanoyltransferase and molecular determinants of substrate selectivity, *J. Biol. Chem. 280*, 738−744.
15. Cordente, A. G., López-Viñas, E., Vázquez, M. I., Swiegers, J. H., Pretorius, I. S., Gómez-Puertas, P., Hegardt, F. G., Asins, G., and Serra, D. (2004) Redesign of carnitine acetyltransferase specificity by protein engineering, *J. Biol. Chem. 279*, 33899−33908.
16. Hsiao, Y., Jogl, G. and Tong, L. (2004) Structural and biochemical studies of the substrate selectivity of carnitine acetyltransferase, *J. Biol. Chem. 279*, 31584−31589.
17. Govindasamy, L., Pedersen, B., Lian, W., Kukar, T., Gu, Y., Jin, S., Agbandje-McKenna, M., Wu, D., and McKenna, R. (2004) Structural insights and functional implications of choline acetyltransferase, *J. Struct. Biol. 148*, 226−235.
18. Cai, Y., Cronin, C. N., Engel, A. G., Ohno, K., Hersh, L. B., and Rodgers, D. W. (2004) Choline acetyltransferase structure reveals distribution of mutations that cause motor disorders, *EMBO J. 23*, 2047−2058.
19. Cronin, C. N. (1998) Redesign of choline acetyltransferase specificity by protein engineering, *J. Biol. Chem. 273*, 24465−24469.
20. Govindasamy, L., Kukar, T., Lian, W., Pedersen, B., Gu, Y., Agbandje-McKenna, M., Jin, S., McKenna, R., and Wu, D. (2004) Structural and mutational characterization of L-carnitine binding to human carnitine acetyltransferase, *J. Struct. Biol. 146*, 416−424.
21. Cronin, C. N. (1997) cDNA cloning, recombinant expression, and site-directed mutagenesis of bovine liver carnitine octanoyltransferase, *Eur. J. Biochem. 247*, 1029−1037.
22. Morillas, M., López-Viñas, E., Valencia, A., Serra, D., Gómez-Puertas, P., Hegardt, F. G., and Asins, G. (2004) Structural model of carnitine palmitoyltransferase I based on the carnitine acetyltransferase crystal, *Biochem. J. 379*, 777−784.
23. Hooft, R. W., Vriend, G., Sander, C., and Abola, E. E. (1996) Errors in protein structures, *Nature 381*, 272.
24. Vriend, G. (1990) WHAT IF: a molecular modeling and drug design program, *J. Mol. Graph. 8*, 52−56.
25. Laskowski, R. A., MacArthur, M. W., Moss, D. S., and Thornton, J. M. (1993) PROCHECK: a program to check the stereochemical quality of protein structures, *J. Appl. Crystallogr. 26*, 283−291.
26. Goodsell, D. S., Morris, G. M., and Olson, A. J. (1996) Automated docking of flexible ligands: applications of AutoDock, *J. Mol. Recognit. 9*, 1−5.
27. Morris, G. M., Goodsell, D. S., Halliday, R. S., Huey, R., Hart, E., Belew, R. K., and Olson, A. J. (1998) Automated docking using a Lamarckian genetic algorithm and an empirical binding free energy function, *J. Comput. Chem. 19*, 1639−1662.
28. Morillas, M., Gómez-Puertas, P., Roca, R., Serra, D., Asins, G., Valencia, A., and Hegardt, F. G. (2001) Structural model of the catalytic core of carnitine palmitoyltransferase I and carnitine octanoyltransferase (COT): mutation of CPT I histidine 473 and

alanine 381 and COT alanine 238 impairs the catalytic activity, *J. Biol. Chem. 276*, 45001−45008.
29. Swiegers, J. H., Dippenaar, N., Pretorius, I. S., and Bauer, F. F. (2001) Carnitine-dependent metabolic activities in *Saccharomyces cerevisiae*: three carnitine acetyltransferases are essential in a carnitine-dependent strain, *Yeast 18*, 585−595.
30. Hassett, R. P., and Crockett, E. L. (2000) Endpoint fluorometric assays for determining activities of carnitine palmitoyltransferase and citrate synthase, *Anal. Biochem. 287*, 176−179.
31. Anderson, R. C. (1998) Carnitine palmitoyltransferase: a viable target for the treatment of NIDDM? *Curr. Pharm. Des. 4*, 1−16.
32. Wagman, A. S., and Nuss, J. M. (2001) Current therapies and emerging targets for the treatment of diabetes, *Curr. Pharm. Des. 7*, 417−450.
33. DeLano, W. L. (2002) *The PyMOL Molecular Graphics System*, DeLano Scientific, San Carlos, CA.

BI0602664